Sustainable Structures
ISSN: 2789-3111 (Print); ISSN: 2789-312X (Online)
http://www.sustain-dpl.com/journal/sust
DOI: 10.54113/j.sust.2026.000102

ORIGINAL ARTICLE

Mechanical properties, microstructural features, and acoustic behaviour of recycled aggregate concrete reinforced with plastic and polypropylene hybrid fibers for sustainable construction

Vijayalakshmi Ramalingam[a,*], Aswin Sriram[a], Geetha Ramalingam[b], Divyah Nagarajan[c], Prakash Ramaiah[d]

[a] Department of Civil Engineering, Sri Sivasubramaniya Nadar College of Engineering, Chennai 603110, India
[b] Department of Biomedical Engineering, Saveetha School of Engineering, SIMATS, Chennai 602105. India
[c] Department of Civil Engineering, PSG Institute of Technology and Applied Research, Coimbatore 641004, India
[d] Department of Civil Engineering, Alagappa Chettiar Government College of Engineering and Technology Karaikudi 630003, India
[*]Corresponding Author: Vijayalakshmi Ramalimgam. Email: vijayalakshmir@ssn.edu.in

Abstract: The increasing demolition of aged infrastructure has significantly raised the generation of recycled aggregates, posing sustainability challenges in construction waste management. Integrating recycled aggregates into concrete production is a potential solution, although they typically exhibit inferior mechanical performance compared to natural aggregates. To overcome this, hybrid fiber reinforcement has gained research interest for improving Recycled Aggregate Concrete (RAC) characteristics. This study examines the performance of RAC reinforced with a combination of plastic and polypropylene fibers used in macro and micro forms respectively to improve resistance against cracking and enhance structural integrity. The concrete was prepared with a 50% replacement of natural aggregates by recycled aggregates, and fiber contents were varied (0.5%, 1%, and 2%). For hybridization, combinations of plastic and polypropylene fibers were tested at three dosage levels: (0.5% PF + 0.5% PP), (0.75% PF + 0.25% PP), and (1.5% PF + 0.5% PP). The impact of fiber type and dosage on mechanical strength, failure patterns, stress strain response, and acoustic emission behavior was investigated. Results showed that the hybrid mix RAC50-PF0.75-PP0.25 yielded superior strength values, achieving 48.56 MPa in compressive strength, 5.19 MPa in splitting tensile strength, and 5.75 MPa in flexural strength, representing improvements of approximately 7%, 5.5%, and 4% respectively over the plain RAC mix.

Keywords: recycled aggregate concrete, hybrid fibers, plastic fiber, polypropylene, acoustic emission, microstructural evaluation

1 Introduction

In recent years, there has been a marked increase in the application of recycled materials within the construction sector, particularly in concrete production aimed at promoting environmental sustainability. Recycled concrete aggregate (RCA) has emerged as a prominent substitute material in this context [1]. The adoption of dry processing methods has enabled the production of recycled aggregates (RA) suitable for both ready-mix and precast concrete applications [2]. Compared to natural

Received: 24 March 2025; Received in revised form: 8 December 2025; Accepted: 8 March 2026

aggregates (NA), RA typically exhibits lower density, higher porosity, elevated water absorption, and an increased crushing index. Moreover, the mechanical fragmentation process involved in their production often [3] induces additional microcracks within the aggregate particles [4]. To further understand the impact of recycled aggregates in concrete applications, researchers have explored Recycled Aggregate Concrete (RAC) combined with alkaline activators. This approach aims to improve mechanical and fundamental properties through enhanced hydration and chemical interactions within the concrete matrix [5]. One study proposed a mix design strategy for alkali-activated concrete incorporating 100% recycled aggregate using ground granulated blast-furnace slag (GGBS), where both the alkalinity level and sodium hydroxide concentration were shown to significantly influence strength development [6]. Additionally, the inclusion of coal ash and treated wastewater with RA has demonstrated potential in producing an environmentally friendly and performance-efficient concrete composite. To facilitate the use of RAC in aggressive environments such as coastal zones, researchers have investigated its durability enhancement through various techniques. Studies have shown that the incorporation of specific mineral admixtures or pre-treatment of recycled aggregates can enhance the density of RAC and improve its resistance to corrosion, making it more suitable for marine applications [7,8]. However, the replacement of natural aggregates with recycled ones, especially when combined with seawater for mixing or curing has been reported to adversely affect both the mechanical performance and long-term durability of the resulting concrete, particularly at higher replacement ratios (50–100%) [9]. To improve the structural integrity of recycled aggregate concrete, various types of fibers, such as steel, plastic, basalt, glass, and polypropylene, each possessing a high elastic modulus have been utilized in different volume fractions to mitigate macro-crack formation. Several studies have highlighted that steel fiber reinforcement can effectively offset the strength deficiencies typically associated with RAC [10,11]. Numerous investigations in recent years have focused on evaluating the structural performance of recycled aggregate concrete reinforced with steel fibers. However, one of the key limitations of steel fibers is their susceptibility to corrosion, which can negatively impact the durability and longevity of concrete elements. As a corrosion-resistant alternative, glass fiber-reinforced polymer (GFRP) bars have been employed, although their anisotropic nature and brittle response under compressive loading present challenges in structural applications [12]**.** Among synthetic fibers, polyolefin types have gained attention due to their high tensile strength, superior chemical stability, and long-term durability, making them well-suited for improving the performance of RAC. Vijayalakshmi et al [13] explored the integration of hybrid fibers into recycled aggregate concrete and reported notable enhancements in both compressive strength and durability metrics. Natural fibers such as jute are currently being studied for their potential role in enhancing the lifespan and durability of concrete elements [14]. Incorporating jute fibers at a dosage of 0.4% has been observed to improve the mechanical performance by approximately 4%, along with noticeable gains in the durability of recycled aggregate concrete[15,16]. Rather than relying on a single type of fiber, the use of hybrid fiber systems typically combining macro fibers with high tensile capacity and micro fibrillated fibers has proven effective in controlling cracks across multiple scales [17]. Such hybrid configurations have been shown to provide a synergistic effect, leading to improved resistance against both early-stage microcracks and later-stage macrocrack propagation [18]. Various natural and synthetic fiber types are under active investigation for their potential use in concrete, particularly to enhance structural longevity and durability [19]. Key factors such as fiber material, dosage (volume fraction), length, and geometric configuration significantly influence the mechanical strength and overall performance of fiber-reinforced concrete [19,20]. The strategy of combining multiple fiber types, rather than using a single reinforcement fiber, has consistently demonstrated improvements in both mechanical strength and durability across various concrete systems including conventional concrete, foam concrete, geopolymer mixtures, and self- compacting concrete [22,23]. Some of the recent research on fiber reinforced recycled aggregate concrete is highlighted in **Table 1**.

Previous experimental efforts clearly indicate that fibers of differing scales and classifications contribute significantly to improving mechanical performance and mitigating crack formation across different loading stages. Given the multi-scale nature of crack development in concrete, incorporating both micro and macro fibers in a hybrid configuration provides a more comprehensive crack-arresting strategy. In hybrid systems, microfibers help delay initial cracking, while macro fibers act to control and bridge wider cracks, collectively improving the toughness and ductility of the concrete matrix [24].

In the case of monofilament fibers, tensile stress is primarily transferred along the fiber's longitudinal axis through elongation or contraction **(Fig. 1(a))**. Conversely, fibrillated fibers disperse stresses in multiple directions due to their branched structure, as illustrated in **Fig. 1(b)**. During the elastic phase of loading, the stress–strain behavior remains linear, reflecting stable internal resistance to deformation [25]. At this stage, fibrillated microfibers play a critical role in delaying the initiation of microcracks. As the loading progresses and the matrix stress exceeds its limit, microcracks begin to form and propagate [26]. Macro fibers become essential at this point by bridging these microcracks and preventing their transition into larger macrocracks. This multidirectional stress redistribution contributes to delaying the formation of major fracture planes [27]. The combined effect of monofilament macrofibers and fibrillated microfibers enhances energy dissipation and suppresses early crack propagation under loading [28]. The crack arresting mechanism of macro and micro fibers is illustrated in **Fig. 2**.

Table 1. Recent literature on FRRAC

S.No	Literature	Fiber	Study parameter	Result
1	Pereiro-Barcelo et al. (2024)[29]	Conventional steel & Recycled steel fiber	Heat resistance and mechanical performance	Recycled fibers showed comparable strength at elevated temperatures; suitable for sustainable use.
2	Chen Htet et al. (2024)[30]	Basalt & Polypropylene fiber	Flexural behaviour with BFRP & SBCB reinforcement	Hybrid fiber system with BFRP/SBCB bars enhanced ductility; new empirical relations proposed.
3	Bao et al. (2025) [31]	Basalt & Glass fiber	Compressive, tensile & flexural strengths; dosage optimization	Notable tensile/flexural gains with glass fibers; peak at 1.5% volume fraction.
4	Xutao et al. (2024)[32]	High-toughness synthetic fiber	Impact response and strain-rate effect	HTRAC displayed superior impact resistance; numerical models developed using SHPB testing.
5	Zhong et al. (2025) [33]	Basalt & Polyacrylonitrile	Flexural fatigue with Weibull analysis	Hybrid mix extended fatigue life; basalt and PANF showed excellent synergy.
6	Mishra &Goel (2025)[34]	Surface treated natural fibers	Surface-modification impact on RAC	Natural fiber coating improved durability and strength; environmentally sustainable approach.
7	Islam et al. (2025) [35]	Nylon fiber	Strength & durability with GGBS	GGBS and nylon fiber synergistically enhanced compressive and flexural capacities.
8	Zhou et al. (2024) [36]	Steel fiber	Fracture properties of ITZ	High steel fiber volume weakened the interfacial transition zone (ITZ); SEM confirmed findings.
9	Zhang et al. (2025) [37]	Steel & Polypropylene fiber	Hybrid effect on autogenous shrinkage	Shrinkage was reduced with 0.5% SF + 1.5 kg/m³ PF; predictive models developed.
10	Li et al. (2024)[38]	Bamboo fiber	Stress-strain behaviour in lightweight concrete	Bamboo fibers improved tensile properties and crack control with minor compressive trade off.

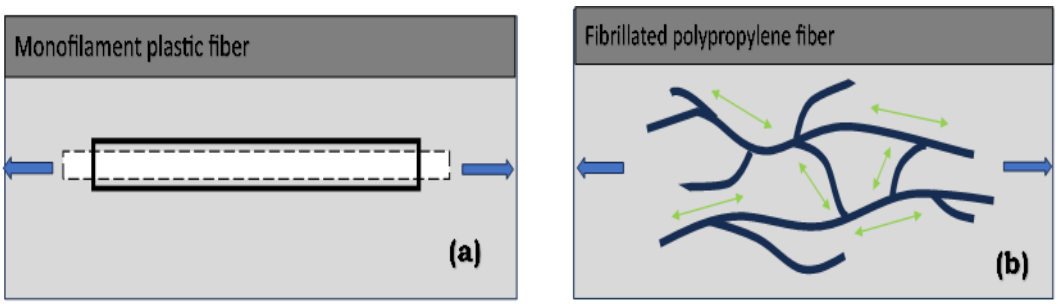

Fig. 1. Stress distribution of macro fiber and fibrillated micro fibers

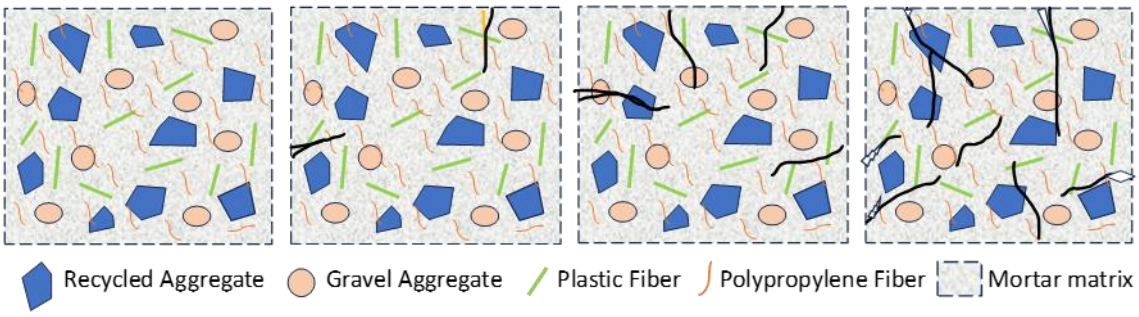

Fig. 2. Crack arresting mechanism of hybrid fiber reinforced concrete

2 Research significance

Extensive studies have been undertaken to assess the mechanical performance of hybrid fiber-reinforced recycled aggregate concrete, particularly through varying fiber types and their combinations. The primary aim of this investigation is to evaluate the influence of macro plastic and micro polypropylene fibers on the structural behavior of RAC. Specific emphasis is placed on understanding the role of these hybrid fibers in crack mitigation through mechanical property evaluation, stress strain characterization, acoustic analysis, and SEM-based microstructural examination. Insights gained from this research are expected to support the broader adoption of RAC in structural applications by improving its reliability and performance.

3 Experimental investigations

This study focuses on assessing the influence of varying replacement levels of recycled coarse aggregate in concrete, reinforced using macro plastic and micro polypropylene fibers applied both individually and in hybrid form. The investigation aims to identify an optimized mix proportion that balances recycled content and fiber dosage to enhance both mechanical properties and microstructural integrity. A schematic overview of the experimental methodology followed is presented in **Fig. 3**.

3.1 Materials

The details of the materials used in the experimental study is discussed below:

Cement: All concrete mixes in this study were prepared using 53-grade Ordinary Portland Cement (OPC), conforming to IS: 12269-1987. The cement was free from lumps, fresh, and stored in moisture-free conditions to maintain its reactivity and consistency.

Natural Coarse Aggregate: Crushed granite obtained from a local quarry was used as the natural coarse aggregate. The material exhibited angular geometry and was screened to retain particle sizes between 4.75 mm and 20 mm. Prior to mixing, aggregates were conditioned to a surface-dry state and verified for compliance with IS: 383-2016 grading standards. Maintaining Saturated Surface Dry (SSD) condition ensured consistency in the water–cement ratio, especially critical when working alongside high-absorption recycled aggregates.

Recycled Coarse Aggregate: Recycled aggregates were prepared by processing M30-grade concrete cubes that had previously undergone mechanical testing. The cubes were first manually broken and then crushed to achieve a desired particle size, while also minimizing the amount of adhered mortar. The processed material was sieved to retain particles within the 4.75 mm to 20 mm size range. These aggregates were collected from controlled on-site concrete waste to maintain uniformity in source quality. Before use, they were thoroughly washed and oven-dried. The relevant physical characteristics of both recycled and natural aggregates are presented in **Table 2**.

Fine Aggregate: The fine aggregate used in this study was locally sourced river sand, classified under Zone II as per IS: 383-2016. The sand was clean, free of deleterious materials such as silt and clay, and demonstrated acceptable gradation properties. Key physical attributes, including specific gravity and fineness modulus, are detailed in **Table 2**. The particle size distribution was verified through sieve analysis, and the resulting gradation curve is illustrated in **Fig. 4**.

Superplasticizer: Polycarboxylate ether (PCE) based water-reducing admixture was incorporated to enhance the workability of the concrete mixtures. The admixture was uniformly dosed at 1% of the

cement weight for all batches, ensuring consistency in fresh properties. Slump values were controlled within the desired range of 75 to 100 mm.

Fibers: To reinforce the recycled aggregate concrete, micro polypropylene fibers and macro plastic fibers were incorporated in varying proportions. Their inclusion aimed to improve mechanical performance and crack resistance. The physical properties of the selected fibers are provided in Table 2, while representative images of all materials used are shown in **Fig. 5**.

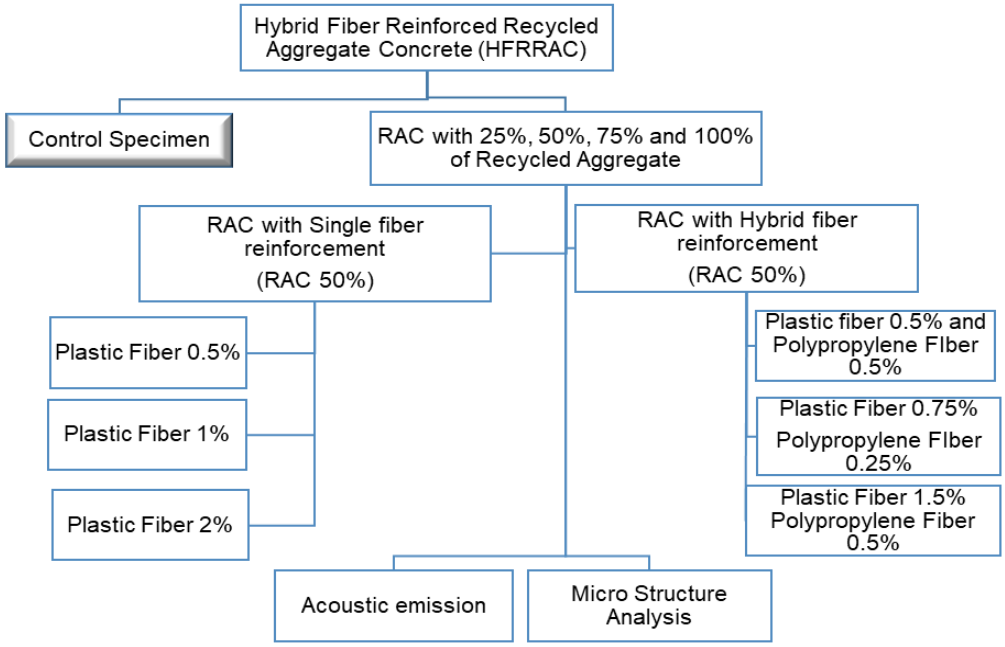

Fig. 3. Methodology of the Hybrid Fiber Reinforced RAC research work

Table 2. Material properties

Property	Natural Aggregate	Recycled Aggregate	Sand (Fine Aggregate)	Plastic Fiber	Polypropylene Fiber
Specific Gravity	2.65	2.35	2.6	0.91	~0.91
Water Absorption (%)	0.5	4.5	1.0	Nil	Nil
Bulk Density (kg/m³)	1600	1350	1450	-	-
Fineness Modulus	-	-	2.75	-	-
Maximum Length (mm)	20	20	4.75	12–50 (length)	6–24 (length)
Shape	Angular	Irregular	Rounded	Monofilament	Fibrillated
Colour	Gray	Light Gray	Light Brown	White/Gray	White
Tensile Strength (MPa)	-	-	-	400–550	350–600
Elastic Modulus (GPa)	-	-	-	3–5	3.5–5

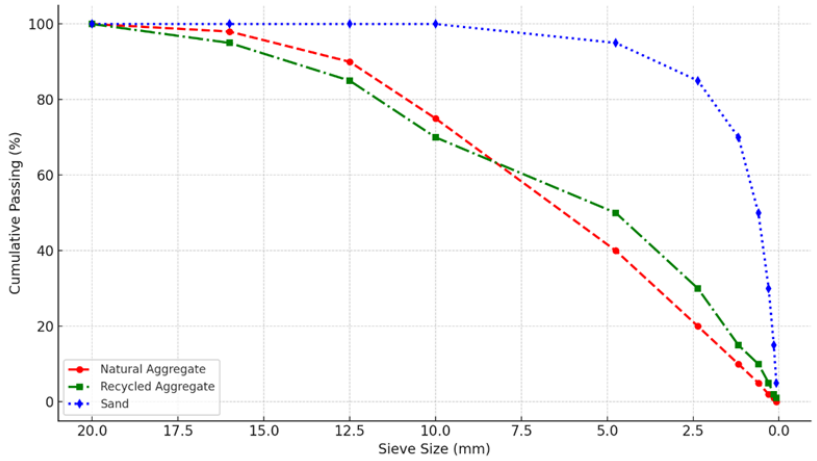

Fig. 4. Gradation curve for coarse and fine aggregate

(a) Recycled aggregate

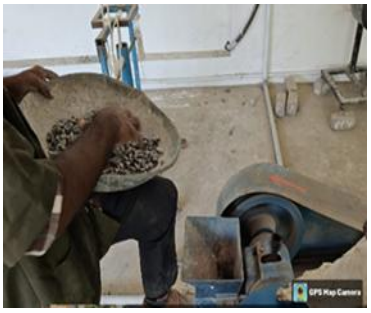

(b) Crushed Aggregate

(c) Natural Aggregate

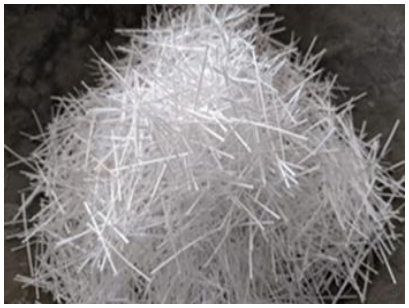

(d) Plastic fiber

(e) Polypropylene Fiber

Fig. 5. Photographic views of the primary materials utilized in this investigation.

3.2 Mix proportion and specimen preparation

Table 3 The mix design specifications for all prepared concrete batches

Specimen ID	Cement (Kg/m3)	Gravel (Kg/m3)	RA (Kg/m3)	Sand (Kg/m3)	Water (Kg/m3)	Plastic (Kg/m3)	PP fiber (Kg/m3)	Admixture (Kg/m3)
Control	690	2400	-	1500	345	-	-	1.6
RAC 25	690	1850	550	1500	345	-	-	1.6
RAC 50	690	1300	1100	1500	345	-	-	1.6
RAC 75	690	550	1850	1500	345	-	-	1.6
RAC 100	690	-	2400	1500	345	-	-	1.6
RAC 50- PF 0.5	690	1300	1100	1500	345	4.95	-	1.6
RAC 50- PF 1	690	1300	1100	1500	345	9.9	-	1.6
RAC 50- PF 2	690	1300	1100	1500	345	19.8	-	1.6
RAC 50- PF 0.5-PP 0.5	690	1300	1100	1500	345	4.95	4.95	1.6
RAC 50- PF 0.75-PP 0.25	690	1300	1100	1500	345	7.425	2.45	1.6
RAC 50- PF 1.5-PP 0.5	690	1300	1100	1500	345	14.85	4.95	1.6

Table 4 Specimen details

Specimen ID	Details of specimen
Control	Control mix with natural aggregate
RAC 25	25% recycled aggregate
RAC 50	50% recycled aggregate
RAC 75	75% recycled aggregate
RAC 100	100% recycled aggregate
RAC 50- PF 0.5	Recycled aggregate 50% and 0.5% plastic fiber
RAC 50- PF 1	Recycled aggregate 50% and 1% plastic fiber
RAC 50- PF 2	Recycled aggregate 50% and 2% plastic fiber
RAC 50- PF 0.5-PP 0.5	Recycled aggregate 50% - 0.5% PF and 0.5 % PP

RAC 50- PF 0.75-PP 0.25	Recycled aggregate 50% - 0.75% PF and 0.25 % PP
RAC 50- PF 1.5-PP 0.5	Recycled aggregate 50% - 1.5% PF and 0.5 % PP

The control mix for this study was prepared using a material ratio of 1:1.64:1.72:0.32:0.01 for cement, sand, coarse aggregate, water, and superplasticizer respectively. The mix design adhered to the guidelines outlined in IS 456:2000 and IS 800. Mixing was carried out in a standard concrete mixer, where all dry components were initially blended for about one minute. Water was then added incrementally, and mixing continued for another two minutes to ensure uniform consistency prior to casting. For the hybrid fiber-reinforced RAC mixtures, the process began with loading cement, fine aggregate, and coarse aggregate into the mixer. This dry blend was mixed for two minutes before water was gradually added. The mixing was continued for another two minutes to ensure uniform hydration. Next, the macro plastic and micro polypropylene fibers were introduced and blended for one more minute. The inclusion of macro plastic fibers and micro-polypropylene fibers is shown in **Fig.6(a&b)** respectively. For each mix design, a set of specimens was cast: three cubes (150×150×150 mm) for compressive strength, three cylinders (150×300 mm) for splitting tensile strength, three for uniaxial compression, and three beams (150×150×750 mm) for flexural strength testing. Slump testing was also conducted immediately after mixing to evaluate workability. The mix proportion for the casted specimen is listed in **Table 3**. Specimen identification followed a structured naming format. The prefix "RAC" denotes recycled aggregate concrete, followed by the replacement percentage of natural aggregate. In the case of fiber-reinforced mixes, the label further specifies the fiber type(s) and dosage. For instance, RAC50–PF1.5–PP0.5 indicates 50% replacement of natural aggregate, combined with 1.5% plastic fiber and 0.5% polypropylene fiber. A full list of specimen identifiers and their configurations is provided in **Table 4**.

(a) Plastic fiber (b) polypropylene Fiber

Fig. 6 The inclusion of macro plastic fibers and micro-polypropylene fibers

3.3 Testing

Table 5 Testing details of specimen

S. No.	Test Type	Test Standard	Specimen Size (mm)
1	Cube Compressive Strength Test	IS 516:1959 [39]	150 × 150 × 150 (cube)
2	Splitting Tensile Strength Test	IS 5816:1999 [40]	150 (Dia) × 300 (height) cylinders
3	Flexural Strength Test	IS 516:1959 [39]	150 × 150 × 750 (beam)
4	Uni-axial Stress-Strain Behaviour	IS 516:1959 [39]	150 (Dia) × 300 (height) cylinders
5	Acoustic Emission (Impedance Tube Test)	ISO 10534-2, ASTM E1050-12	29.5 mm & 99.5 mm diameter samples
6	Digital Image Processing & Microstructure Analysis	(Imaging analysis techniques)	Image data from cracked specimens

A comprehensive set of tests was conducted to evaluate the mechanical strength, acoustic performance, and microstructural features of the prepared concrete specimens. **Table 5** provides a detailed overview of the testing procedures, including the applicable standards and specimen sizes adopted for each experimental evaluation. The mechanical tests—including compressive strength,

splitting tensile strength, and flexural strength—were carried out in accordance with IS 516:1959 [39] and IS 5816:1999 [40].To examine the uni-axial stress–strain response, cylindrical specimens were subjected to displacement-controlled loading, with deformation data captured using linear variable differential transformers (LVDTs) and strain gauges connected to a data acquisition system. The experimental configuration used for mechanical testing is depicted in **Fig. 7.** The acoustic absorption behaviour of the hybrid fiber-reinforced RAC was measured using the Impedance Tube method, conforming to ISO 10534-2 and ASTM E1050-12, across a range of frequencies. Additionally, Scanning Electron Microscopy (SEM) and Digital Image Processing (DIP) were employed to assess internal microstructural features, crack evolution, and fiber-matrix interactions—thereby supporting the mechanical findings with visual and quantitative micro-level evidence.

(a) Cube Compression test

(b) Splitting tensile strength test

(c) Flexural strenght test

(d) Unia axial compression test

Fig. 7. Mechanical test of hybrid fiber reinforced recycled aggregate concrete

3.4 Acoustic analysis using impedance tube test

Acoustic performance, referring to the control of sound transmission through materials and structures, is crucial in applications ranging from noise insulation to the design of acoustically tuned environments such as auditoriums and studios. In many construction projects, soundproofing has become a functional necessity. Conventionally, concrete is not regarded for its sound-absorbing capabilities, typically exhibiting a low absorption coefficient (α) in the range of 0.05 to 0.10 [41]. The sound absorption coefficient (α) quantifies a material's ability to absorb incident sound energy, with higher values indicating improved sound insulation capabilities [42]. In this study, both the absorption and transmission loss characteristics of fiber-reinforced RAC were evaluated using the Impedance Tube method, following standardized protocols outlined in ISO 10534-2 and ASTM E1050-12. These internationally accepted procedures enable accurate and reproducible measurement of sound absorption across a broad frequency spectrum. The impedance tube technique relies on analyzing sound wave

reflections and transmissions within a rigid cylindrical tube using a calibrated sound source and sensitive microphones. The method accommodates sample diameters of 29.5 mm and 99.5 mm, facilitating frequency measurements ranging from 50 Hz to 6,300 Hz. A schematic diagram of the experimental setup is provided in **Fig. 8.**

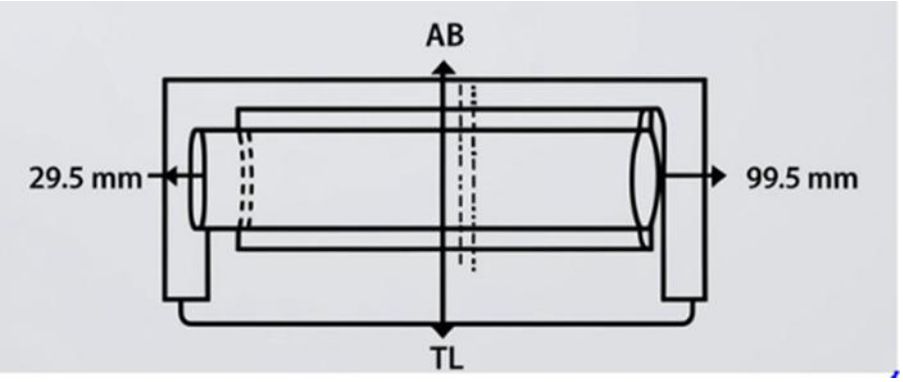

Fig. 8. Schematic diagram of acoustic emmission test setup

3.5 Digital image processing technique

The methodology adopted for Digital Image Processing (DIP) and microstructural evaluation is outlined below. Concrete specimens incorporating both monofilament and fibrillated fibers were selected for imaging. High-resolution internal microstructure images were obtained using Scanning Electron Microscopy (SEM) and optical microscopy at multiple magnification levels. These images focused on key features such as fiber distribution, bonding between fibers and the cement matrix, and the quality of embedded recycled aggregates. Post-capture, DIP techniques—including noise filtering, image thresholding, edge detection, morphological filtering, and crack width quantification—were applied to enhance image clarity and extract microstructural features.

Following are the types of microstructure analysis that was performed using digital image processing: (i) Fracture Surface Characterization: Examines crack initiation and propagation patterns in relation to fiber distribution and orientation within the concrete matrix. (ii) Quantitative Microstructure Assessment: DIP was used to compute parameters such as fiber alignment, porosity levels, void distribution, crack length, and crack density. (iii) Comparative Statistical Analysis: Extracted features (e.g., fiber orientation, crack geometry) were statistically evaluated across samples to assess distribution uniformity and compare the effectiveness of monofilament and fibrillated fibers.

4 Results and Discussion

4.1 Fresh property

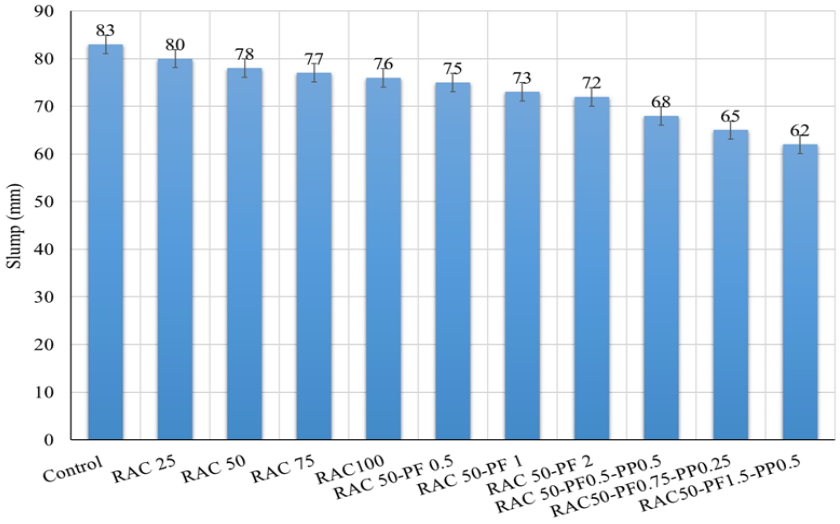

Fig. 9. Slump cone test

Fig. 10. Workability of RAC using slump cone test

The workability of the concrete mixtures was assessed through slump tests **(Fig. 9)**, and the results are illustrated in **Fig. 10**. The control mix recorded the highest slump at 83 mm, reflecting superior workability. As the percentage of recycled aggregates increased, a consistent decline in slump values was observed: 80 mm for RAC 25, 78 mm for RAC 50, 77 mm for RAC 75, and 76 mm for RAC 100. This decrease is primarily attributed to the greater water absorption capacity and irregular particle shape of recycled aggregates, which limit the availability of free water during mixing.

The incorporation of plastic fibers had a notable impact on the fresh properties of RAC. For RAC 50 mixes, increasing fiber content from 0.5% to 2% led to a drop in slump values—from 75 mm to 72 mm and further to 68 mm. This trend is attributed to the enhanced interlocking among fibers and their tendency to trap water, thereby reducing the effective water available for workability. In mixes with hybrid fibers—comprising both macro plastic and micro polypropylene fibers—workability further declined. The slump values for RAC 50–PF0.5–PP0.5, RAC 50–PF0.75–PP0.25, and RAC 50–PF1.5–PP0.5 were recorded as 68 mm, 65 mm, and 62 mm, respectively. This sharper reduction is a combined effect of dual fiber systems, which increase internal friction and limit flowability. Overall, the results reveal a clear compromise between increased recycled content and fiber dosage versus the ease of mixing and placement in fresh concrete.

4.2 Failure pattern

Equations The failure behaviour of uni axial compression cylinders for four different cases has been analyzed in detail. The four types of specimens include (i) RAC with 50% recycled aggregate (ii) RAC with 0.5 % plastic fiber (iii) RAC with 2% plastic fiber and (iv) RAC with 0.75PF -0.25PP Hybrid fiber is shown in **Fig. 11-14**. The RAC 50 control specimen, containing 50% recycled aggregate without any fibers, exhibited a typical brittle failure pattern as shown in **Fig.11(a-d)**. During the cube compression test, the specimen developed distinct vertical splitting cracks that initiated at the loaded surfaces and propagated downward along the specimen's height. Due to the absence of fibers to restrict these cracks, the cracks quickly widened and led to a collapse of the concrete matrix [25]. The concrete spalling observed was significant, with large pieces detaching from the surface. In the splitting tensile test, the specimen failed along a vertical crack plane that extended continuously through the height of the cylinder. These observations confirm that the recycled aggregate content reduces the interfacial bonding strength, thereby making the matrix susceptible to splitting tensile failure and brittle compressive failure[15]. The fracture surface was coarse and irregular, indicating abrupt energy release during failure.

(a) Splitting tensile test (b) Beam flexure test

(c) Cube Compression Test (d) Uniaxial Test Specimen

Fig. 11. RAC 50% tested specimen

When 0.5% plastic fibers were added to RAC 50, the failure pattern shifted from brittle to a more controlled response as shown in **Fig.12(a-c)**. In the cube compression test, while vertical cracks still developed, their width was significantly reduced compared to the control specimen[29]. The plastic fibers effectively bridged these cracks, delaying their propagation and reducing spalling of the surface concrete. In the splitting tensile tests, the fibers distributed the applied tensile stress across the crack faces, slowing crack development and resulting in a more gradual failure[23]. During uniaxial compression loading, the presence of fibers reduced the size of spalled concrete pieces and enhanced the specimen's ability to sustain post-peak load capacity[43]. Overall, the inclusion of 0.5% plastic fibers transformed the failure mode from purely brittle splitting to a shear-dominated, fiber-bridged crack propagation, reflecting improved toughness and crack arresting ability.

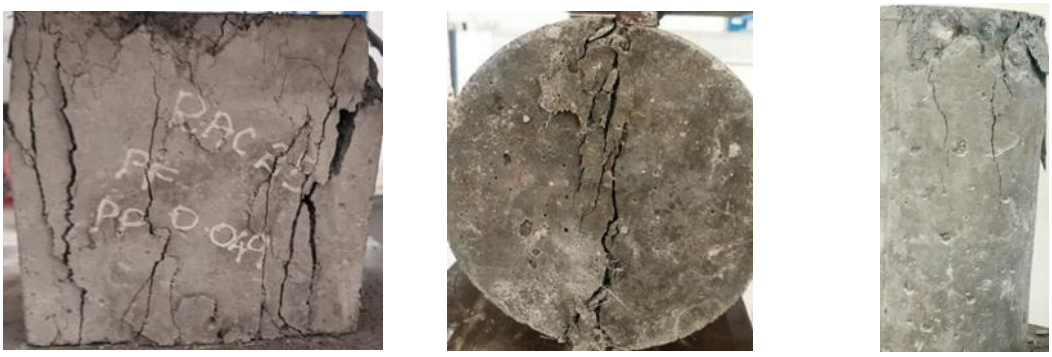

(a) Cube test (b) Splitting tensile test (c) Uniaxial compression test

Fig. 12. RAC with 0.5% plastic fiber

With an increased fiber content of 2%, the RAC 50 specimen displayed further modifications in its failure behaviour as shown in **Fig.13(a-c)**. In compression testing, the fibers enhanced the crack-bridging mechanism, limiting the crack opening and propagation even under peak load conditions. The crack patterns in these specimens were more diffuse, and the spalling was minimal compared to lower fiber dosages[15]. The increased fiber volume fraction improved the energy dissipation capacity, allowing the specimen to undergo larger deformations before final failure. In the splitting tensile test, the fibers delayed the development of critical crack planes and enhanced the residual load-carrying capacity after crack initiation[25]. Despite potential challenges in workability at higher fiber dosages, the test results clearly show that the fibers succeeded in converting the sudden brittle failure into a more gradual, shear-induced crack growth. The observed crack planes were narrower and interconnected, indicative of enhanced post-crack behaviour and stress redistribution due to the higher fiber content.

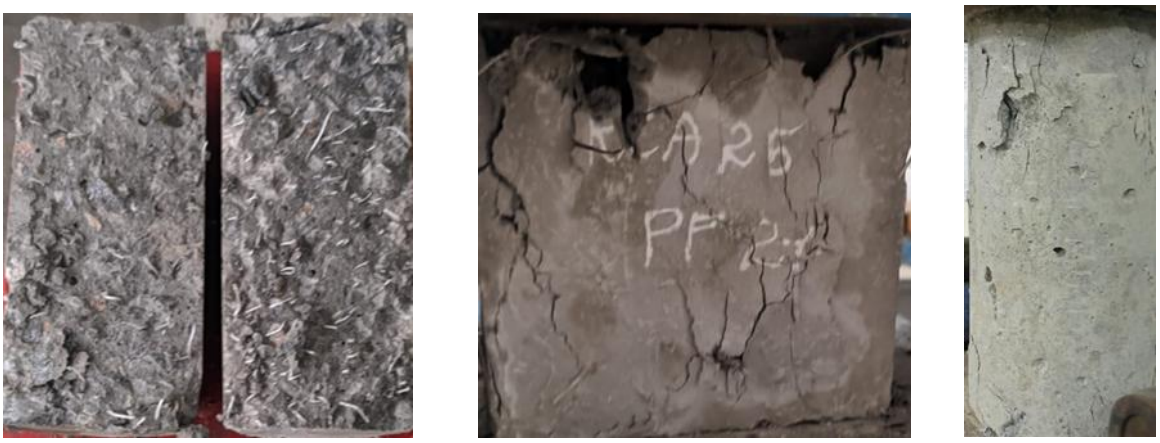

(a) Splitting tensile test (b) Cube Compression test (c) Unial compression test

Fig. 13. RAC with 2 % plastic fiber

The hybrid fiber-reinforced RAC 50 specimens exhibited the most pronounced improvement in failure behavior as shown in **Fig.14(a-c)**. During the cube compression tests, the hybrid system resulted in a synergistic crack-arresting effect. The micro polypropylene fibers effectively restrained the formation of micro-cracks in the early stages of loading, while the macro plastic fibers bridged the macro-cracks that developed at higher stress levels [44]. This dual mechanism significantly enhanced the specimen's toughness and delayed the formation of dominant crack planes. In the splitting tensile test, the hybrid fiber system promoted a uniform distribution of stresses across the specimen, leading to a slower and more controlled crack propagation. During uniaxial compression testing, the hybrid fibers provided enhanced crack-bridging and stress transfer capabilities[45]. The failure surfaces were less abrupt and exhibited a combination of shear and flexural failure modes, suggesting a transition from brittle to ductile behavior. The integrity of the cracked specimens was notably higher, and the crack widths remained limited even under large deformations[30]. The hybrid fiber combination not only improved crack control but also enhanced the energy dissipation and post-peak toughness of the recycled aggregate concrete.

(a) Cube test (b) Splitting tensile test (c) Uniaxial compression test

Fig. 14. RAC with hybrid fiber reinforcement

4.3 Uni axial stress-strain behaviour

The typical stress-strain response of the recycled aggregate concrete (RAC 50) reinforced with plastic fibers is illustrated in **Fig. 15**. In the initial stage (OA), the curve shows a linear elastic response where the stress is directly proportional to strain, indicating that the concrete is in the elastic deformation phase with minimal internal cracking. As the applied load increases, the curve transitions into the stable crack propagation stage (AB), wherein microcracks begin to develop and propagate progressively. This stage is marked by a slight deviation from linearity, reflecting the onset of inelastic deformation and microstructural adjustments in the concrete matrix. The peak load-carrying capacity is achieved at the

end of the AB segment, representing the maximum compressive strength of the RAC 50 specimen. For the control specimen without fibers, this value was 40.85 MPa, while it decreased progressively with higher recycled aggregate content to 39.25 MPa, 38.0 MPa, 36.5 MPa, and 34 MPa for 25%, 50%, 75%, and 100% replacement levels, respectively. This reduction is primarily attributed to the presence of adhered old mortar on recycled aggregates and their irregular geometry, which hinder the bonding and introduce micro-defects.

After the peak load, the stress-strain curve enters the rapid crack propagation stage (BC), taking a concave trajectory towards the stress axis. At this stage, the inclusion of plastic fibers plays a significant role in bridging developing cracks, mitigating their opening, and delaying the formation of major crack planes. This bridging effect of the fibers is evident in the reduced crack width and the more gradual load decline in the post-peak region compared to control specimens lacking fiber reinforcement. Subsequently, the curve transitions into the unstable crack propagation and failure stage (CD), where the stress exhibits a pronounced drop as the specimen approaches complete failure. The fibers continue to contribute by providing limited resistance to crack widening until they are eventually pulled out of the matrix as the concrete loses its load-bearing capacity. Overall, the addition of plastic fibers to RAC 50 notably improves the ductility and energy absorption capacity of recycled aggregate concrete, effectively mitigating the inherent brittleness typically associated with higher recycled aggregate contents. This improved behavior is consistent with observations reported in the literature, highlighting the beneficial role of fiber reinforcement in controlling crack propagation and enhancing post-peak load-bearing performance of recycled aggregate concrete. The effect of different experimental parameters on the stress strain response of RAC is explained in the below section.

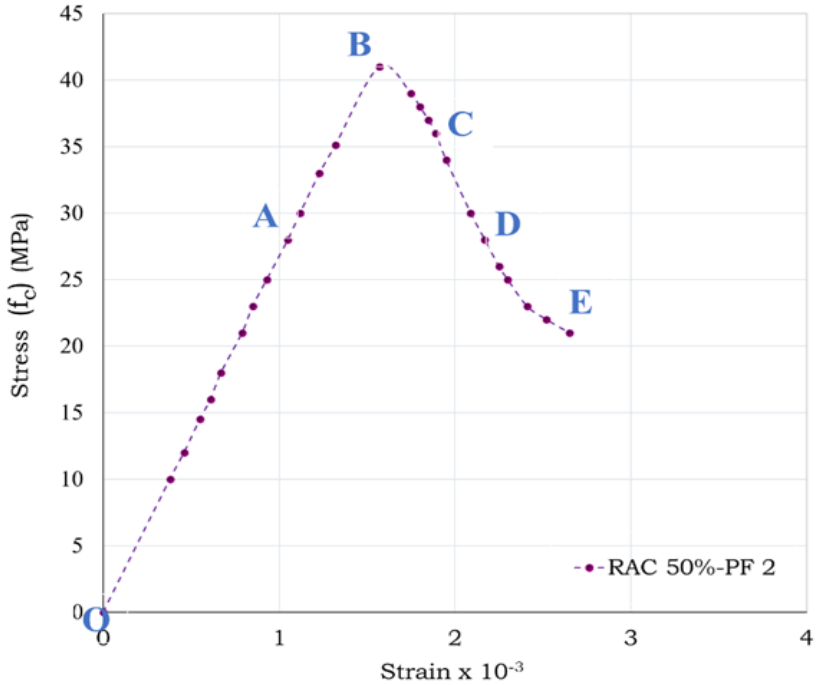

Fig.15. Stress strain plot of RAC 50 with single fiber

4.3.1 Recycled aggregate replacement rate

As shown in **Fig. 16**, the stress–strain responses of concrete specimens with varying recycled aggregate (RA) replacement levels exhibit a clear trend of decreasing peak stress with increasing RA content [46]. The control specimen achieved the highest peak compressive strength of approximately 41 MPa, which progressively decreased to around 39 MPa, 38 MPa, 36.5 MPa, and 34 MPa for RA replacement rates of 25%, 50%, 75%, and 100%, respectively. The stress–strain curves for all mixes initially display a linear elastic region, followed by a deviation from linearity as microcracks initiate and propagate within the matrix [47]. Previous studies have established that the adhered old mortar on RA surfaces creates weak zones that compromise the bond between the recycled aggregates and the new cement matrix, thereby reducing load-bearing capacity [48]. Moreover, the irregular shape and

angularity of recycled aggregates increase the presence of stress concentrators, promoting crack development under compressive loads [49]. The higher porosity and greater water absorption of RA further exacerbate this strength reduction by altering the internal moisture balance, leading to more porous and less dense microstructures in the hardened concrete [50].

Cui et al. [25] have specifically highlighted two primary contributors to this decline in strength: (i) the existence of pre-existing microcracks and flaws within the recycled aggregates, and (ii) the formation of a thin layer of old mortar around the aggregates that introduces additional interfaces in the concrete. These interfaces act as planes of weakness, promoting crack initiation and propagation at lower stress levels. Furthermore, the combined work of Bayraktar et al. (2021) [51] demonstrated that the incorporation of fly ash and polypropylene fibers with recycled aggregates can partially offset the reduction in compressive strength, achieving compressive strengths close to 60 MPa for RAC mixes with 25% and 50% replacement. However, in the current study, without the addition of such supplementary cementitious materials or fibers, the decrease in strength is more pronounced beyond 50% replacement, consistent with the work of Bayraktar et al. and further corroborated by the progressive downward shift of the peak stress observed in the graph. Importantly, despite this strength reduction, the stress–strain curves for RAC mixes still display a gradual post-peak softening behavior, suggesting that recycled aggregate concrete retains a certain degree of ductility and energy absorption capacity [52]. This behavior, although less pronounced than that of the control mix, indicates the potential for recycled aggregate concrete to be employed in structural applications if appropriately modified such as through the inclusion of fibers or pozzolanic additives to counteract the negative effects of higher RA content. These observations are in line with recent literature emphasizing the role of RA in modifying concrete's mechanical response while highlighting the need for hybrid reinforcement strategies to maintain structural integrity in RAC mixes with higher RA content [53].

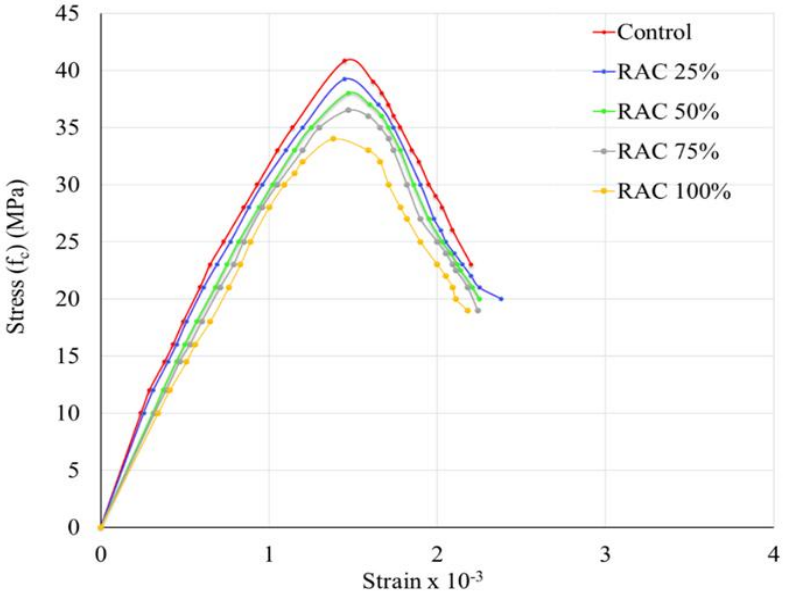

Fig.16. Stress strain plot of control and RAC

4.3.2 Effect of macro fiber reinforcement

The stress–strain behavior of RAC 50% reinforced with varying dosages of plastic fiber (0.5%, 1%, and 2%) is shown in **Fig. 17**. The curves reveal that the addition of plastic fibers significantly modifies the mechanical response of recycled aggregate concrete, particularly enhancing the post-peak region and the overall ductility[19]. Initially, all curves exhibit a linear elastic region up to the peak load, indicating that the presence of plastic fibers does not markedly alter the elastic stiffness of the RAC 50 mix. However, beyond the elastic limit, the role of fibers becomes more pronounced. As the stress approaches the peak, the plastic fibers begin to bridge developing micro-cracks, thereby delaying the onset of macro-crack propagation[12]. This bridging action of the fibers results in a more gradual reduction in load-carrying capacity after the peak, as evident in the softened descending branch of the

curves compared to the plain RAC.

The recorded peak stresses for the RAC 50% specimens reinforced with 0.5%, 1%, and 2% plastic fibers are approximately 39.12 MPa, 40.05 MPa, and 41.0 MPa, respectively. This progressive increase in peak stress with fiber content is attributed to the enhanced crack-bridging capacity of plastic fibers with higher modulus of elasticity, which effectively redistribute stresses and delay crack opening. The curvature of the stress–strain plot post-peak further highlights the improved toughness of the fiber-reinforced RAC[54]. In this plastic region, fibers are activated, controlling crack propagation and enhancing energy absorption capacity[55]. Moreover, it is observed that the initial slope of the stress–strain curve increases with the fiber dosage, indicating an improvement in the stiffness of the composite[56]. However, the sensitivity of peak strain to fiber addition is reduced, consistent with literature observations by Zhang et al. [57], which reported similar improvements in stiffness and reduced strain sensitivity due to fiber reinforcement. Koksal et al. (2022) [58] further noted that the incorporation of macro fibers improves ductility and toughness, confirming the present findings. Overall, the inclusion of plastic fibers in RAC 50% contributes to higher peak compressive strength, enhanced stiffness, and improved post-peak ductility. These results underscore the potential of plastic fiber reinforcement to mitigate the inherent brittleness of recycled aggregate concrete, making it more suitable for structural applications that require improved toughness and energy dissipation capacity.

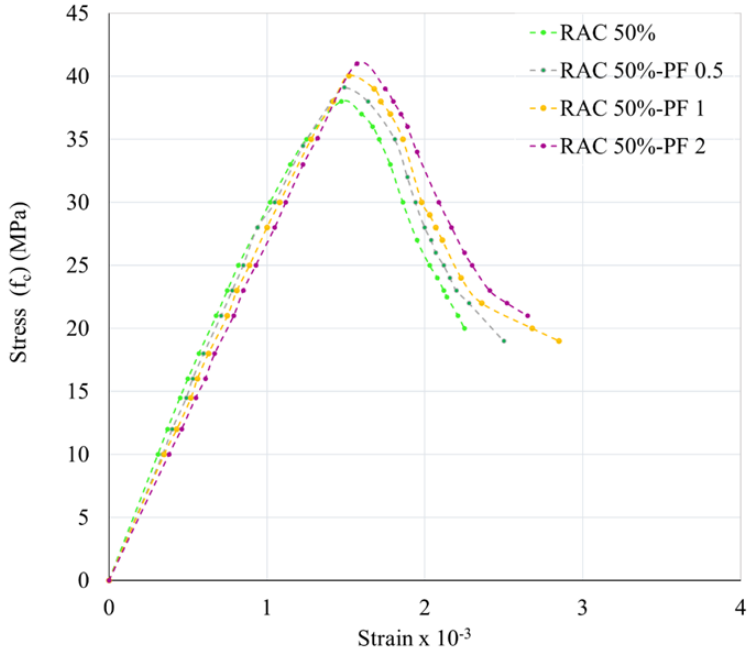

Fig. 17. Stress strain plot of PF reinforced RAC 50%

4.3.3 Effect of hybrid fiber reinforcement

The incorporation of hybrid fibers, comprising both macro-plastic fibers and micro-polypropylene fibers, has a profound impact on the mechanical response of recycled aggregate concrete (RAC), particularly in mitigating brittleness and enhancing post-cracking behavior[24]. The stress–strain response of RAC 50% with hybrid fiber reinforcement is depicted in **Fig. 18**. Initially, all curves in **Fig. 18** show a linear elastic region up to the peak load, signifying that the presence of hybrid fibers does not notably affect the elastic stiffness of the concrete[25]. Beyond this linear region, however, the influence of hybrid fibers becomes evident. As the applied load increases and reaches the peak stress, microcracks begin to form within the matrix[27]. At this stage, the fibrillated polypropylene fibers play a key role in arresting the propagation of microcracks by dissipating stresses across multiple directions, thereby delaying the coalescence of these microcracks into macro cracks[28].

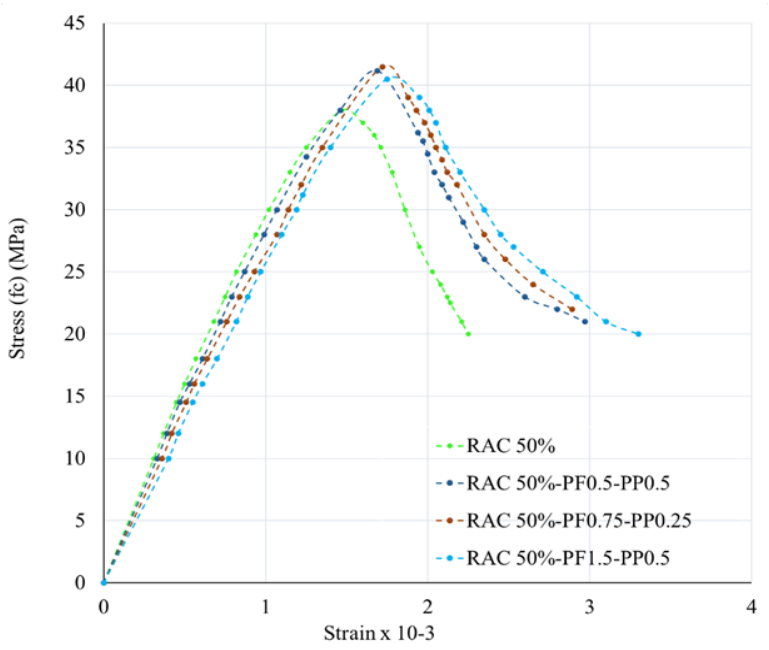

Fig. 18. Stress strain plot of hybrid FRRAC 50%

Simultaneously, the macro-plastic fibers become active in bridging these developing microcracks, effectively delaying the formation of dominant crack planes. This bridging mechanism not only prolongs the crack propagation process but also enhances the energy absorption capacity of the composite material. Consequently, the descending branch of the stress–strain curve is less steep compared to the control or single-fiber specimens, indicating a more ductile failure mode and improved toughness in the hybrid fiber-reinforced RAC. The peak stresses recorded for the hybrid fiber-reinforced RAC 50% specimen vary depending on the fiber dosage and combination. Notably, the presence of both macro and micro fibers significantly enhances the strain capacity and post-peak behavior, resulting in a more gradual and sustained load drop compared to specimens with only macro or micro fibers. These findings corroborate the observations of Xu et al. [18], reported a slower stiffness degradation rate with increasing fiber content, and Zhang et al. [32], documented that hybrid fiber reinforcement reduces the stress drop in the post-peak region, thereby enhancing the plastic deformation capacity of the composite. The crack-arresting synergy of the macro and micro fibers observed in the present study is also consistent with the findings of previous research. The macro fibers effectively bridge larger crack openings, while the micro fibers help distribute localized stresses and control the development of smaller cracks in the early loading stage. This dual mechanism not only mitigates the reduction in strength typically associated with recycled aggregates but also imparts a more ductile and reliable failure mode to the composite.

4.4 Mechanical strength of HFRRAC

The mechanical performance of the hybrid fiber-reinforced recycled aggregate concrete (HFRRAC) was investigated by evaluating the cube compressive strength, splitting tensile strength, and flexural strength for different fiber combinations and replacement levels of recycled aggregate. The peak compressive stress, splitting tensile stress, flexural stress and modulus of elasticity are listed in **Table 6**. The variation of these mechanical properties is shown in **Fig. 19**., **Fig. 20**., and **Fig. 21** respectively.

Table 6 Stress strain values of recycled aggregate concrete

Specimen ID	Axial compressive stress (fc') N/mm2	Splitting Strength (fst) N/mm2	Flexure Strength (fr) N/mm2	Modulus of Elasticity (Ec) N/mm2
Control	40.56	2.76	4.1	27.58
RAC 50	38.79	2.56	3.75	26.97
RAC 50- PF 0.5	42	3.23	4.12	28.06

RAC 50- PF 1	43.12	3.45	4.23	28.43
RAC 50- PF 2	39.12	3.1	4.15	27.08
RAC 50- PF 0.5-PP 0.5	42.43	3.16	4.23	28.20
RAC 50- PF 0.75-PP 0.25	43.45	3.34	4.3	28.54
RAC 50- PF 1.5-PP 0.5	37.98	2.56	3.89	26.68

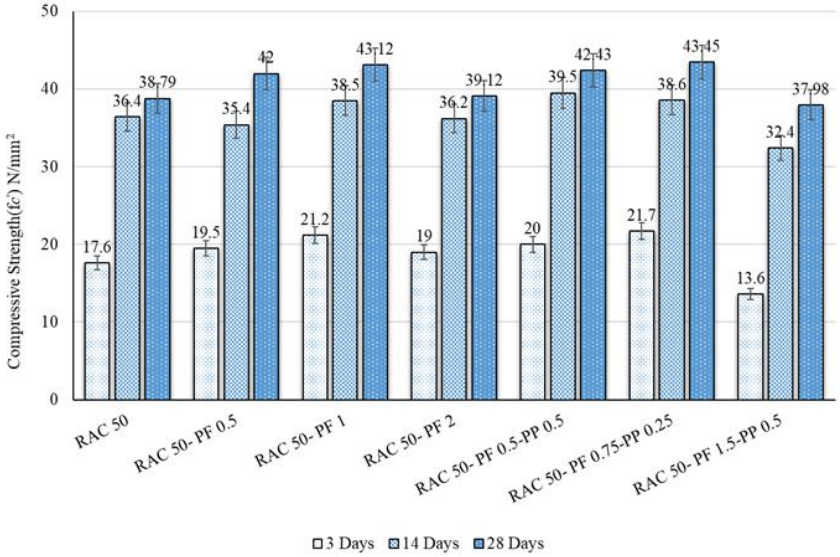

Fig. 19. Cube compressive Strength of hybrid fiber reinforced RAC

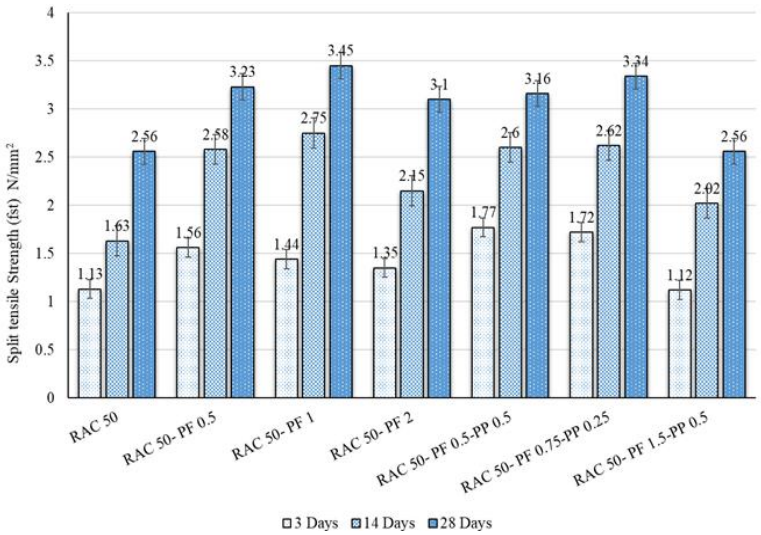

Fig. 20. Splitting tensile Strength of hybrid fiber reinforced RAC

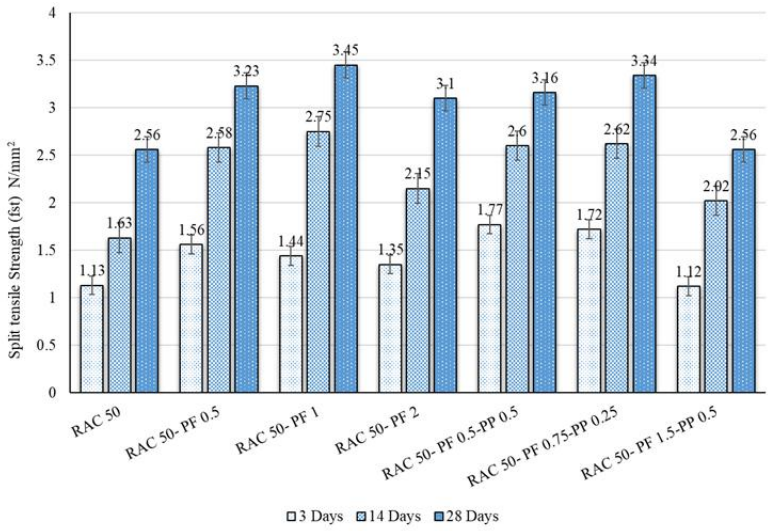

Fig. 21. Flexural strength of hybrid fiber reinforced RAC

The compressive strength of the control specimen was found to be 40.56 MPa. The incorporation of 50% recycled aggregate (RAC 50) led to a reduction in compressive strength to 38.79 MPa due to the presence of adhered mortar and increased porosity in recycled aggregates. The inclusion of plastic fibers (PF) enhanced the compressive strength of RAC 50. Specifically, RAC 50-PF 0.5 exhibited a compressive strength of 42 MPa, and RAC 50-PF 1 further improved it to 43.12 MPa. However, beyond a fiber dosage of 1%, the compressive strength showed a slight decline (RAC 50-PF 2 at 39.12 MPa), possibly due to fiber agglomeration and poor dispersion in the matrix[59]. The splitting tensile strength followed a similar trend. The control specimen achieved 2.76 MPa, whereas RAC 50 had a slightly reduced value of 2.56 MPa. Adding 0.5% plastic fibers increased the splitting tensile strength to 3.23 MPa, while 1% plastic fibers further improved it to 3.45 MPa. Beyond 1% PF dosage, the splitting tensile strength marginally declined (3.1 MPa for RAC 50-PF 2). Hybrid fiber mixes demonstrated enhanced performance compared to single-fiber mixes. RAC 50-PF 0.75-PP 0.25 exhibited the highest splitting tensile strength of 3.34 MPa, underscoring the synergistic effect of combining macro-plastic and micro-polypropylene fibers in resisting crack initiation and propagation.

Flexural strength, a key parameter for structural applications, also improved with fiber inclusion. The control specimen had a flexural strength of 4.1 MPa, which decreased slightly to 3.75 MPa for RAC 50 due to the weaker interfacial transition zone of recycled aggregates. The inclusion of 0.5% and 1% PF led to flexural strengths of 4.12 MPa and 4.23 MPa, respectively. Hybrid fiber systems further improved the flexural strength, with RAC 50-PF 0.75-PP 0.25 reaching 4.3 MPa which is about an 8% increase over the control mix. These results demonstrate that the inclusion of hybrid fibers effectively mitigates the negative impact of recycled aggregates on mechanical properties. The synergistic bridging effect of micro-polypropylene fibers (arresting micro-cracks) and macro-plastic fibers (arresting macro-cracks) enhances the load transfer capacity and toughness of HFRRAC. The findings align with previous research, which suggests that while recycled aggregates inherently reduce compressive strength, the addition of fibers compensates for this drawback by improving ductility and crack resistance [60]. In summary, optimal mechanical performance in HFRRAC was achieved with a hybrid fiber dosage of 0.75% plastic fiber and 0.25% polypropylene fiber. Excessive fiber content, however, can lead to reduced strength due to fiber clustering and reduced workability. Therefore, carefully balanced hybrid fiber combinations provide an effective means to enhance the mechanical behaviour of recycled aggregate concrete.

4.4.1 Regression analysis and emperical correlation

Figure labels must be sized in proportion to the image, sharp, and legible. A detailed regression analysis was conducted to derive empirical correlations between compressive strength (f_c') and key mechanical parameters—namely, splitting tensile strength (f_{st}), flexural strength (f_r), and modulus of elasticity (E_c)—for hybrid fiber-reinforced recycled aggregate concrete mixtures. The experimentally

obtained splitting tensile strength values (f_{st}) were also evaluated against predictions from established design standards, including ACI 318 [61], JSCE-07 [62], JCI-08 [63], and AS 3600-18 [64] and given by Eq. (1-4) respectively. The following empirical correlations were proposed by the above codes:

The following empirical correlations were proposed by the above codes:

$$f_{st} = 0.35\sqrt{f_c'} \quad (1)$$

$$f_{st} = 0.44\left(f_c'\right)^{0.5} \quad (2)$$

$$f_{st} = 0.13\left(f_c'\right)^{0.85} \quad (3)$$

$$f_{st} = 0.44\sqrt{f_c'} \quad (4)$$

The experimental results align closely with these codal equations, as evident in the comparative plots shown in **Fig.22**. From regression analysis of the present data (**Fig. 23**.), a new empirical equation Eq. (5) specific to HFRRAC was developed:

$$f_{st} = 0.45\sqrt{f_c'} \quad (R^2 = 0.952) \quad (5)$$

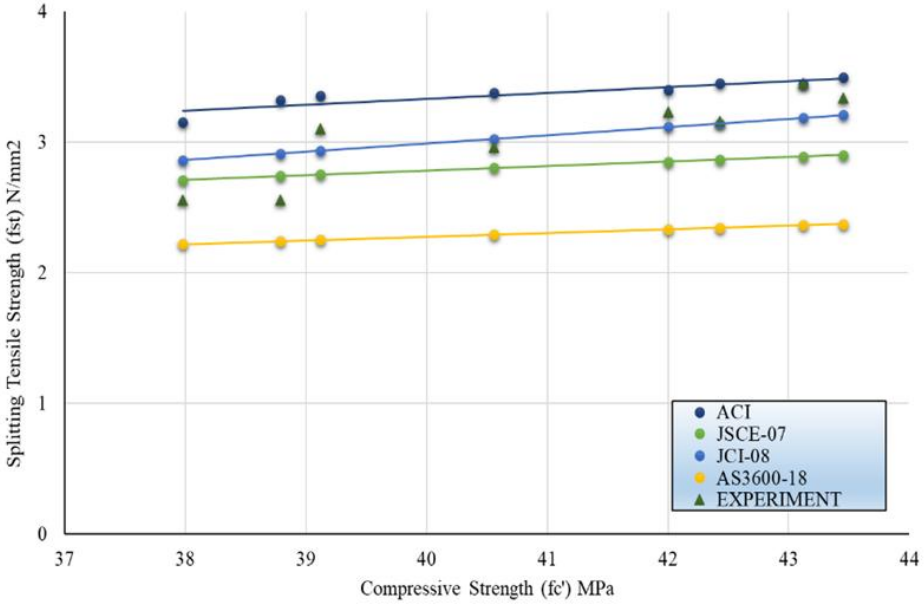

Fig. 22. Comparison of splitting tensile strength with standard codal values

Similarly, flexural strength (f_r) was correlated with compressive strength using standard code formulations such as ACI-318, Eurocode-2 EC-04, NZS3101 is given in Eq. (6-8) respectively.

$$f_r = 0.62\sqrt{f_c'} \quad (6)$$

$$f_r = 0.435\left(f_c'\right)^{2/3} \quad (7)$$

$$f_{st} = 0.6\sqrt{f_c'} \quad (8)$$

A comparison between the experimentally determined flexural strength and the compressive strength correlation models from established codes is illustrated in **Fig. 24**. The plot demonstrates a strong alignment between the experimental data and the predictions made by standard code formulations. Based on the observed trend for hybrid fiber-reinforced recycled aggregate concrete (HFRRAC), a new empirical equation relating flexural strength to compressive strength has been developed, as shown in **Fig. 25** and expressed in Eq. (9).

$$f_{st} = 0.58\sqrt{f_c'} \quad (9)$$

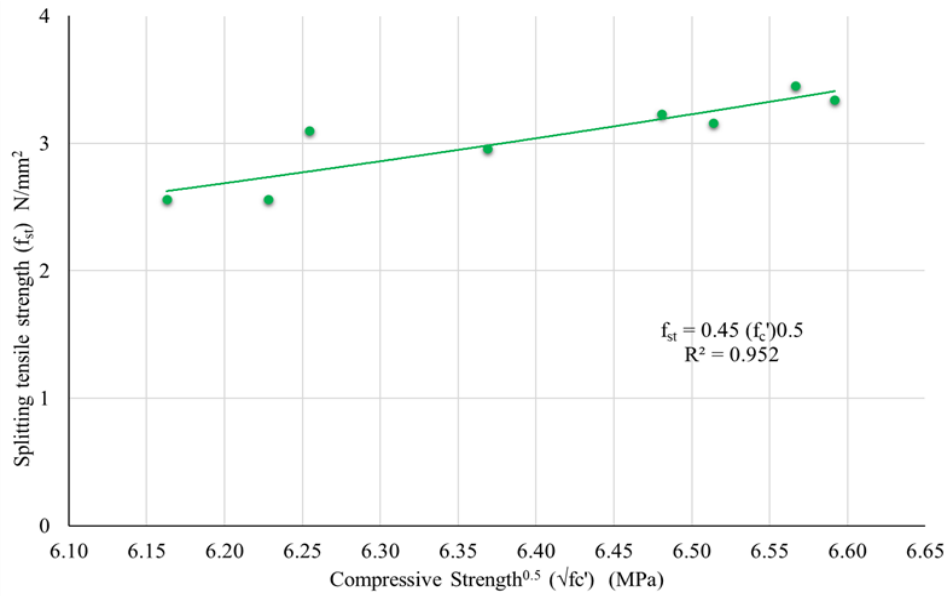

Fig. 23. Regression plot of splitting tensile strength

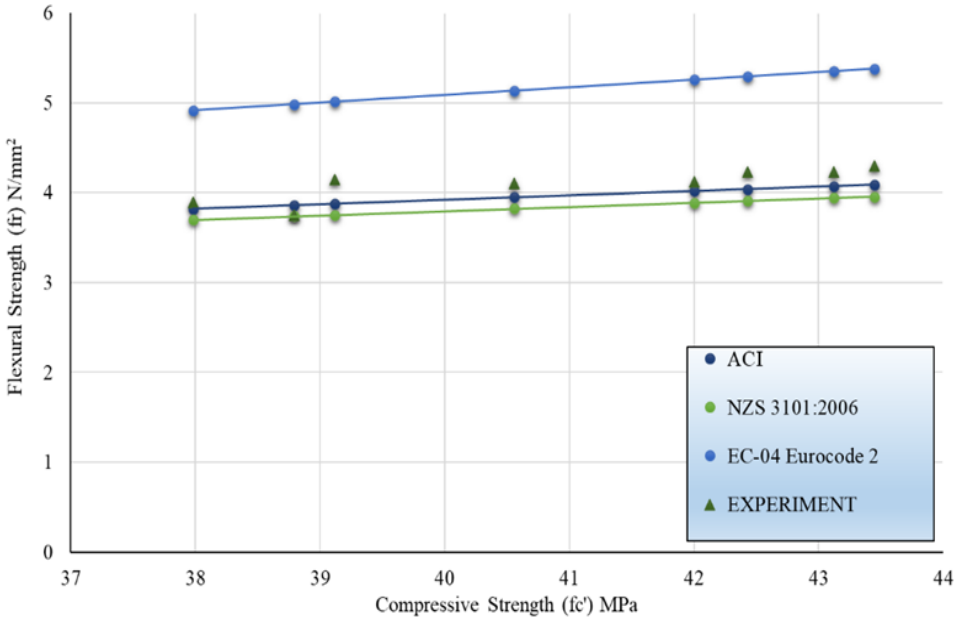

Fig. 24. Comparison of flexural strength with standard codal values

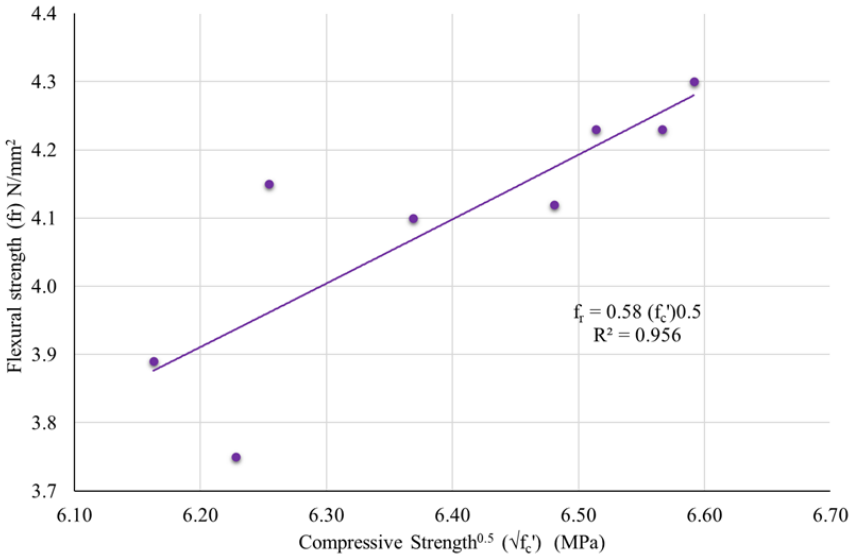

Fig. 25. Regression plot of flexural strength

A linear regression analysis was conducted to formulate an empirical relationship between the modulus of elasticity (E_c) and compressive strength (f_c'). The resulting correlation, which demonstrated a high coefficient of determination (R^2 = 0.99), is illustrated in **Fig. 26**. Equations (10) through (13) present the expressions recommended by design standards such as ACI 318, Eurocode 2 (EC-04), CSA A23.3-04, and NZS 3101 for estimating modulus of elasticity based on compressive strength. A comparative evaluation of the present experimental results with these codal predictions is shown in **Fig. 27**. As evident from the figure, the experimental data aligns closely with the standard code-based correlations. An empirical equation specific to hybrid fiber-reinforced recycled aggregate concrete (HFRRAC) is proposed and provided as Eq. (14)

$$E_c = 4.73\sqrt{f_c'} \tag{10}$$

$$E_c = 4.7\sqrt{f_c'} \tag{11}$$

$$E_c = 4.5\sqrt{f_c'} \tag{12}$$

$$E_c = 3.32\sqrt{f_c'} + 6.9 \tag{13}$$

$$E_c = 4.33\sqrt{f_c'} \tag{14}$$

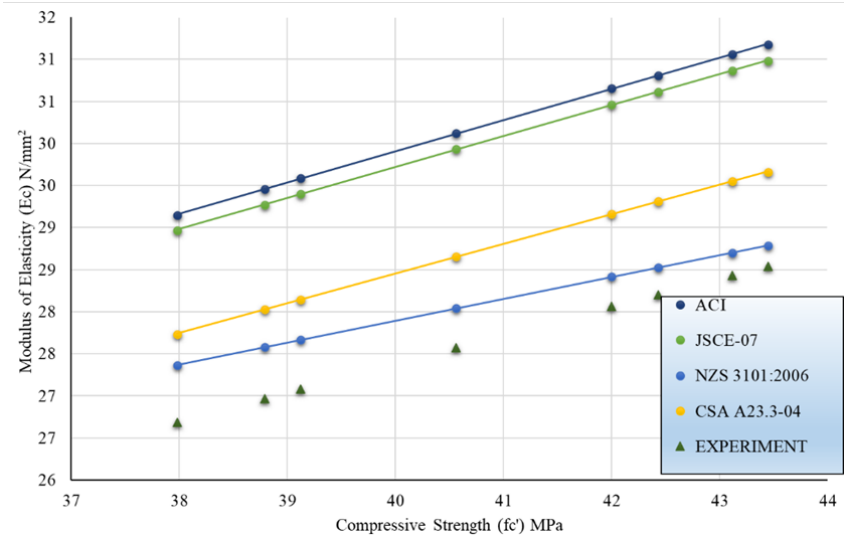

Fig. 26. Comparison of elastic modulus with standard codal values

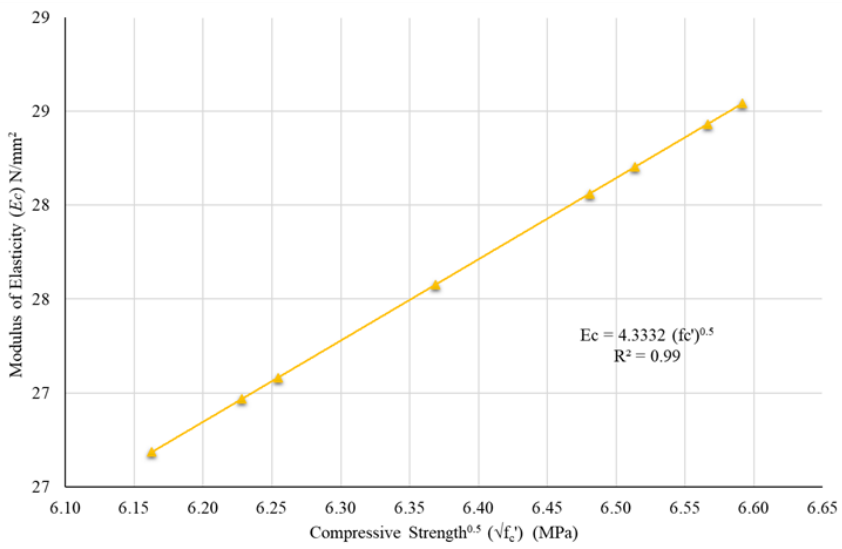

Fig. 27. Regression plot of elastic modulus

4.4.2 Comparative Performance of Hybrid Fiber-Reinforced RAC and literature Studies

The compressive strength data demonstrate clear trend with fiber dosage (**Fig.28**). The present experimental results (Plastic + PPF fibers) consistently show compressive strengths between 35 and 45 MPa across fiber contents of 0–2%. This suggests that hybrid fiber reinforcement effectively maintains compressive strength even with increased fiber dosages. Comparatively, data from Kumari et al. (2023)[65] with steel and glass fibers report the highest compressive strengths, reaching nearly 55 MPa at a 2% fiber content, indicating the significant contribution of steel fibers with high modulus. Azandariani et al. (2024) [66] and Zhang et al. (2024) [67] also show notable strength enhancements, particularly at 1–2% fiber content. Wang et al. (2024) [68] data indicate a linear improvement in compressive strength up to about 3% fiber content, emphasizing the effectiveness of high-modulus fibers in bridging macro cracks. Overall, the trend confirms that steel-based fiber reinforcement generally offers higher compressive strength, but the plastic + PPF hybrid fiber mix in the present study also provides competitive compressive performance, suggesting its potential for sustainable structural applications.

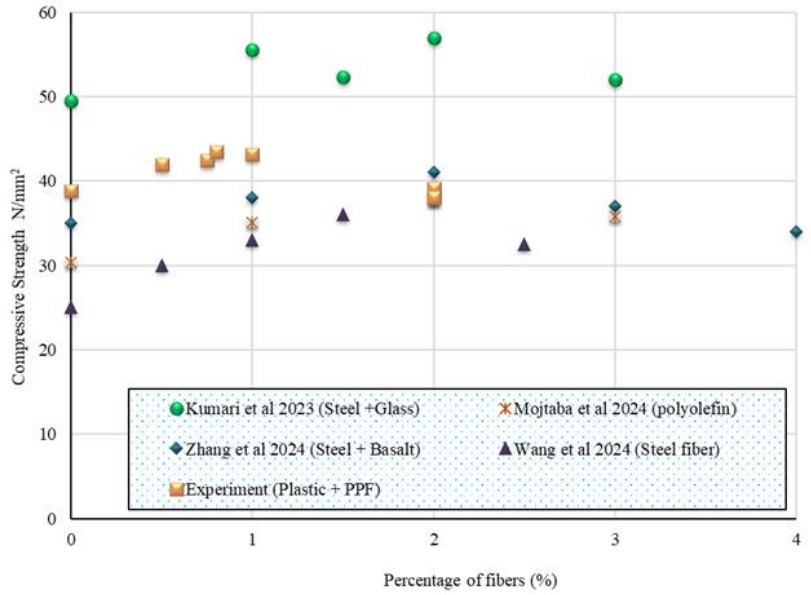

Fig. 28. Comparison of experimental compressive strength with previous research

The comparison of splitting tensile strength with the previous research is shown in **Fig. 29**. The experimental hybrid fiber RAC (Plastic + PPF) shows splitting tensile strengths ranging from 2.5 to 3.5

MPa. With the inclusion of hybrid fibers, an increase of up to 15% over the baseline RAC tensile strength was observed. The literature data show a similar positive trend. Cui et al. (2023) [35] and Kumari et al. (2023) [65] present the highest splitting tensile strengths (around 4 MPa) at 1–2% fiber content. Zhang et al. (2024) [67] and Ouni et al. (2022) [45] report moderate improvements, aligning closely with the present hybrid fiber data. The experimental hybrid fiber RAC's performance parallels that of Ouni et al. and Zhang et al., emphasizing the bridging effect of plastic and polypropylene fibers even though they typically exhibit lower tensile moduli than steel Fibers. This comparison suggests that while steel-based fibers still dominate in tensile strength enhancement, the hybrid plastic–PPF mix in this study provides a viable alternative with competitive tensile performance.

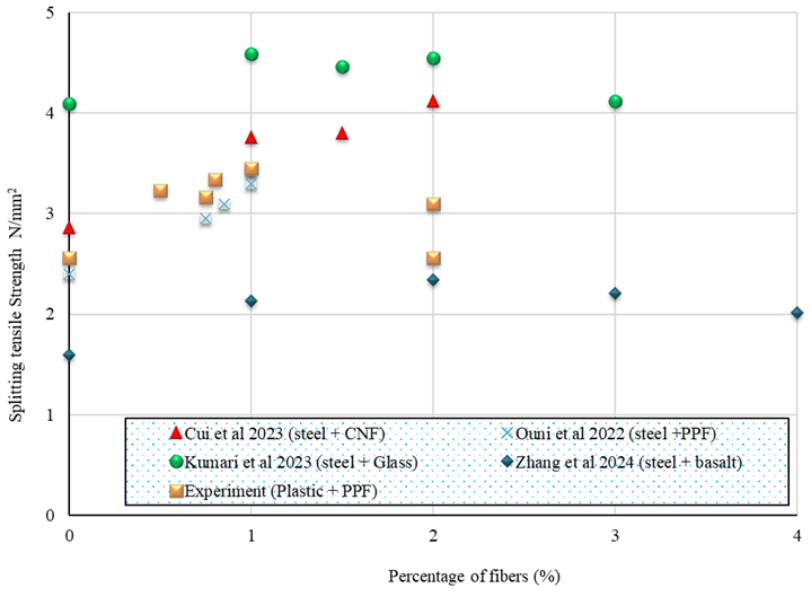

Fig. 29 Comparison of splitting tensile strength with previous research

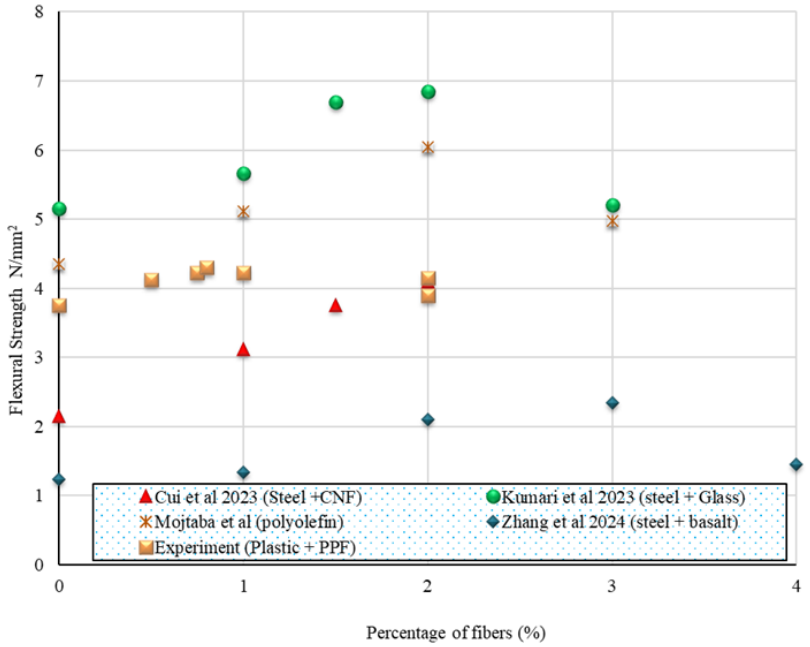

Fig. 30 Comparison of flexural strength with previous research

The comparison of flexural strength with the previous research is shown in **Fig. 30**. The present experimental data show flexural strengths between 3 and 4.5 MPa across fiber dosages up to 2%. This confirms that hybrid fibers help arrest crack propagation and improve post-cracking toughness. Kumari et al. (2023) [65] and Azandariani et al. (2024) [66] report the highest flexural strengths (up to 6–7 MPa), reflecting the excellent bridging and toughness imparted by steel-based or polyolefin fibers. Cui

et al. (2023) [35] and Zhang et al. (2024) [67] exhibit more moderate improvements, similar to the trends observed for splitting tensile strength. In the present study, the hybrid Plastic + PPF system consistently outperformed the control RAC in flexural strength, reinforcing the role of micro and macro fibers in controlling crack widths and delaying macro crack formation. However, the hybrid fiber system's peak flexural strength remains slightly below the values achieved with steel-based fibers, highlighting the difference in fiber stiffness and crack-bridging capabilities.

It can be concluded that all data sets, including the present experimental RAC, show an initial increase in mechanical properties (compressive, splitting tensile, and flexural strength) with fiber content up to about 1–1.5%. Beyond this, there is a slight decrease, likely due to fiber clustering, poor dispersion, and workability. Steel-based fibers (steel + glass, steel + basalt, etc.) consistently achieve higher mechanical performance due to their superior modulus of elasticity and crack-bridging capabilities. The present experimental hybrid system (plastic + PPF), while lower in ultimate strength, shows a well-balanced behaviour and confirms the viability of using recycled polymer-based fibers in sustainable concrete. Despite the marginally lower peak strengths, the hybrid fiber mix in this study offers an eco-friendly alternative to steel fiber systems, especially for moderate-strength structural applications where recycled aggregate content is prioritized.

4.5 Acoustic emission study

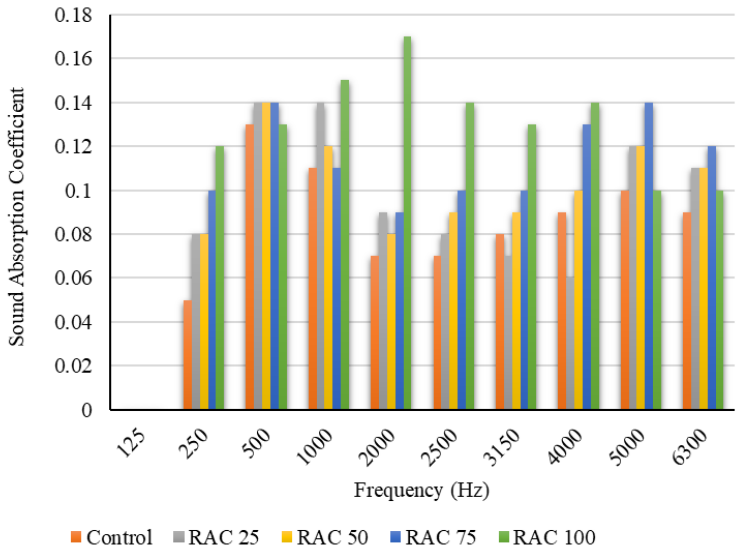

Fig. 31. Sound absorption Coefficient for Recycled Aggregate Concrete

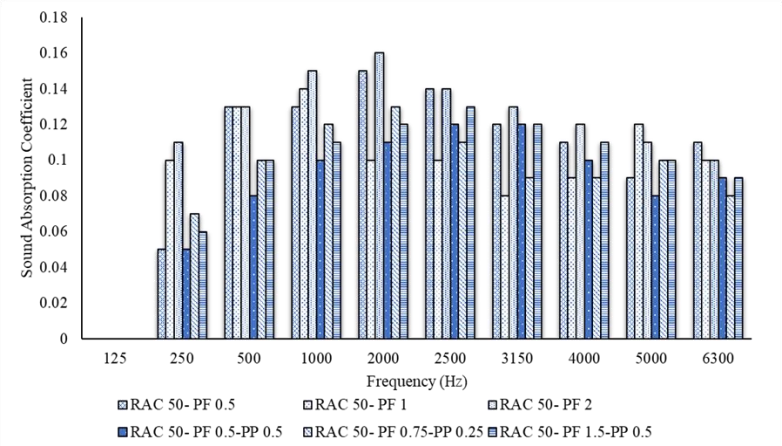

Fig. 32. Sound absorption Coefficient for Fiber reinforced Recycled Aggregate Concrete

The sound absorption and transmission loss of RAC with added fibers were determined using an Impedance Tube Test according to ISO 10534-2 and ASTM E 1050-12. Samples of recycled aggregate

concrete (RAC) with different fiber inclusions were tested and the plot for sound absorption coefficients (α) for different recycled aggregate concrete specimens and fiber reinforced RAC specimen are shown in **Fig. 31** and **Fig. 32** respectively. The coefficient values are listed in **Table 7**.

The behavior of concrete in terms of sound absorption coefficients, as evaluated using the **Table 7**, reflects significant variation based on the inclusion of recycled aggregate concrete (RAC) and supplementary fibres. Conventional relatively low sound absorption across the entire frequency range, which aligns with its dense, homogenous structure. Such materials primarily reflect sound due to their minimal porosity and lack of specific sound-dampening features. In contrast, the addition of RAC and further modifications with additives like plastic fibers (PF) and polypropylene (PP) significantly influence acoustic properties. Concrete mix with 50% RAC and combinations of PF and PP exhibit improved sound absorption, particularly at higher frequencies, which can be attributed to the increased voids and microstructural heterogeneity introduced by these materials. For instance, RAC 50 with PF 1.5 and PP 0.5 showed enhanced absorption coefficients across multiple frequencies, highlighting its potential for applications requiring noise mitigation. Higher proportions of RAC, such as RAC 75 and RAC 100, show progressively better absorption characteristics at mid and high frequencies compared to conventional concrete. This is likely due to the inherent irregularities and increased porosity of RAC. However, at lower frequencies, the variations are less pronounced, which indicates that the effectiveness of these materials in sound absorption is frequency-dependent and more suitable for environments where higher-frequency noise predominates.

When compared to conventional concrete, RAC mixtures, especially those modified with PF and PP, demonstrate superior performance in sound absorption without compromising structural efficiency. The inclusion of fibers and polymers provides additional pathways for sound wave dissipation, enhancing the material's effectiveness in reducing reverberation and improving acoustic comfort. Among the tested combinations, RAC 50 with PF 1.5 and PP 0.5 emerges as one of the most effective configurations, achieving a balance between structural performance and acoustic benefits. Overall, modified RAC, particularly with fiber and polymer additives, proves to be a better alternative to conventional concrete for applications where sound absorption is a priority. These findings are aligned with the principles outlined in ISO 10534-2 and ASTM E 1050-12, which emphasize the importance of material composition and microstructural factors in determining acoustic performance. This makes RAC with appropriate modifications a compelling choice for modern construction needs, especially in settings like auditoriums, highways, and urban areas where noise control is critical.

Table 7 Sound absorption coefficient of recycled aggregate concrete

Frequency (Hz)	Control	RAC 25	RAC 50	RAC 75	RAC 100	RAC 50- PF 0.5	RAC 50- PF 1	RAC 50- PF 2	RAC 50- PF 0.5-PP 0.5	RAC 50- PF 0.75-PP 0.25	RAC 50- PF 1.5-PP 0.5
125	0	0	0	0	0	0	0	0	0	0	0
250	0.05	0.08	0.08	0.1	0.12	0.05	0.1	0.11	0.05	0.07	0.06
500	0.13	0.14	0.14	0.14	0.13	0.13	0.13	0.13	0.08	0.1	0.1
1000	0.11	0.14	0.12	0.11	0.15	0.13	0.14	0.15	0.1	0.12	0.11
2000	0.07	0.09	0.08	0.09	0.17	0.15	0.1	0.16	0.11	0.13	0.12
2500	0.07	0.08	0.09	0.1	0.14	0.14	0.1	0.14	0.12	0.11	0.13
3150	0.08	0.07	0.09	0.1	0.13	0.12	0.08	0.13	0.12	0.09	0.12
4000	0.09	0.06	0.1	0.13	0.14	0.11	0.09	0.12	0.1	0.09	0.11
5000	0.1	0.12	0.12	0.14	0.1	0.09	0.12	0.11	0.08	0.1	0.1
6300	0.09	0.11	0.11	0.12	0.1	0.11	0.1	0.1	0.09	0.08	0.09

4.6 Digital image processing of HFRRAC

Currently, research in the area of automatic fracture detection on various surfaces using digital image analysis is quite extensive [69]. Most of this work emphasizes threshold-based selection and image processing techniques. In this study, the digital images were standardized to 256 × 256 pixels to streamline processing and maintain consistency, albeit with a slight trade-off in data detail. Each image is represented by three color channels red, green, and blue (RGB) where each pixel’s intensity is an integer between 0 and 255. For grayscale images, this intensity ranges from 0 (black) to 255 (white).

After resizing, the images are converted from RGB to grayscale and subsequently transformed into binary images, where pixels are assigned a value of either 0 (black) or 1 (white). This binary conversion facilitates the identification of edges using an advanced edge detection algorithm implemented in MATLAB, which efficiently converts all detected edges into binary representations. Once edges are detected, several morphological operations—clean, close, spur, and bridge—are employed to minimize noise and re-connect fragmented cracks [70].

Following these morphological treatments, connected-component labelling is performed, wherein each continuous region in the image is assigned a unique label. This process helps in recognizing distinct objects and their attributes within the image [71]. The final step involves analyzing these object attributes, which are critical for differentiating actual cracks from noise. These attributes also form the basis for further processing with neural networks or fuzzy logic-based fracture detection methods. Ultimately, the processed images and extracted attributes are displayed for validation and interpretation [72]. **Fig. 33**. shows the digital image of RAC 25 PF 0.5, which primarily contains macro plastic fibers. In this image, most of the region is colored red, indicating the absence of micro cracking in these zones. However, due to the limited number of fibers in the matrix, there is inadequate stress redistribution across the cross-section, resulting in the accumulation of stress in localized regions. Consequently, the major crack planes emerge more readily, emphasizing the importance of hybrid fiber systems in ensuring more uniform stress distribution.

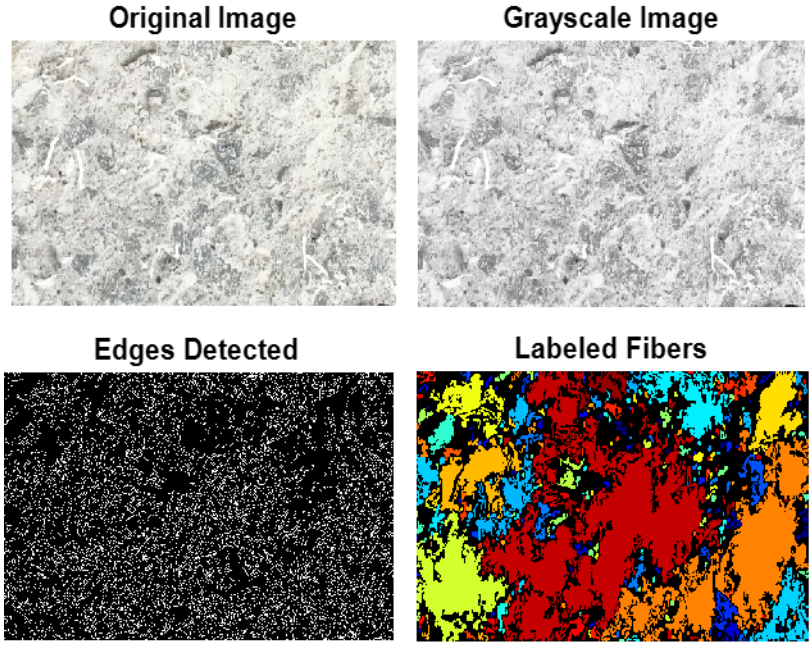

Fig. 33. RAC with 0.5% plastic fiber

Fig.34. shows the digital image of RAC 25-PF 1, which illustrates the development of secondary cracks represented by the blue-colored regions. These secondary cracks are primarily attributed to the presence of micro polypropylene fibers, which effectively control the formation and propagation of micro cracks by arresting them at an early stage [71]. The uniform distribution of these secondary cracks across the concrete matrix indicates the improved elasticity and stress distribution provided by the hybrid fiber system.

Fig. 35. depicts the digital image of RAC 50-PF 1.5-PP 0.5 along a cracked region. Here, the yellow regions correspond to the major crack planes, while the blue regions denote the secondary crack zones. The presence of macro plastic fibers around these major crack planes facilitates bridging across the cracked regions, thereby reducing stress concentrations and improving the overall crack resistance of the concrete [72]. This bridging effect significantly contributes to delaying the progression of micro cracks into macro cracks.

These observations underscore the synergistic effect of micro and macro fibers in enhancing the toughness and crack-resisting behavior of HFRRAC [73]. The combination of polypropylene and

plastic fibers not only delays the formation of major crack planes but also dissipates stress more evenly throughout the matrix[74]. This dual mechanism ultimately contributes to improved durability and mechanical performance of recycled aggregate concrete, supporting its viability for structural applications.

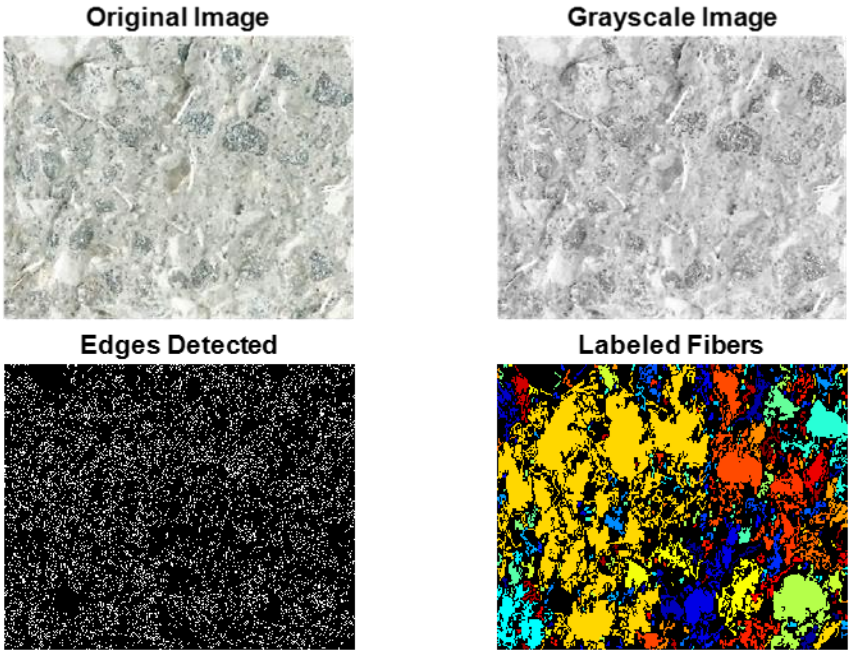

Fig. 34. Digital image of HFRC with 1% plastic fiber

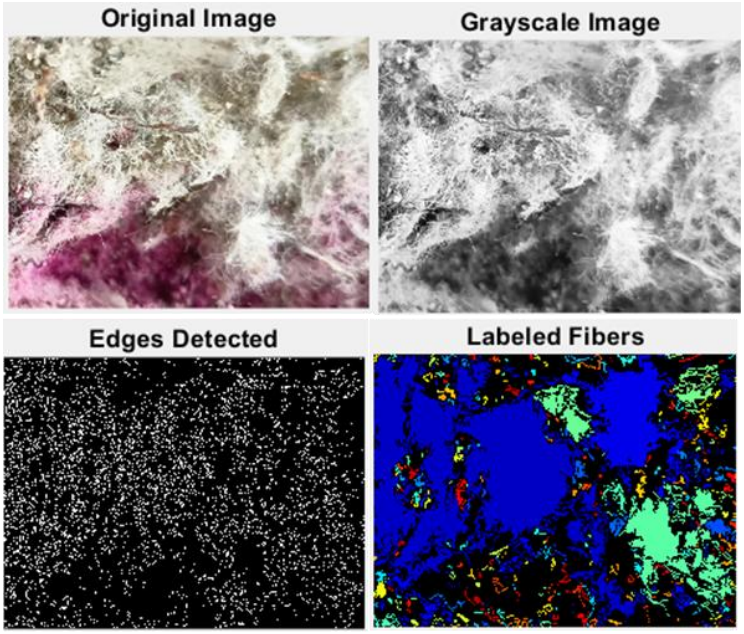

Fig. 35. Digital image of Hybrid fiber reinforced Concrete with excess macro fibers

4.7 Microstructure analysis

Using scanning electron microscopy (SEM), the microstructural properties of samples with and without fibers were investigated. Essential understanding and explanation of the hydration process and interactions and effects of fiber distribution, incomplete hydration processes, and macro-mechanical properties were given by the SEM study results.

4.7.1 Control concrete

To understand the influence of recycled aggregate and hybrid fiber on the behaviour of concrete samples, micro structure analysis was carried out using Scanning Electron Microscope (SEM). The control concrete samples showed the presence of hydration product, number of micro cracks and interface transition zone (ITZ) [74]. The hydration product mainly include calcium silicate, calcium hydroxide, the C-S-H gel are formed by the reaction of calcium oxide with cabon , silica, alumina and form C-S-H gel. The hydration product also contains a needle or rod like ettringites [75]. Cracks are formed in the ITZ zone due to the shrinkage and deformation of hydration products, aggregate and mortar paste. The dense C-S_H gel forms a three dimensional, tightly bonded compact structure which plays a major role in the strength of concrete. the hydration product also has calcium Hydroxide CH which tends to accumulate between the mortar pate and aggregate which results in the weak ITZ zone. In control sample, large number of CH crystals are present which results in the porous microstructure and large number of voids and pores in the sample. The SEM image of control sample showing the porous matrix with voids and heterogenous surface with micro cracks and ITZ between the aggregate and cement mortar is shown in **Fig. 36(a-d)**

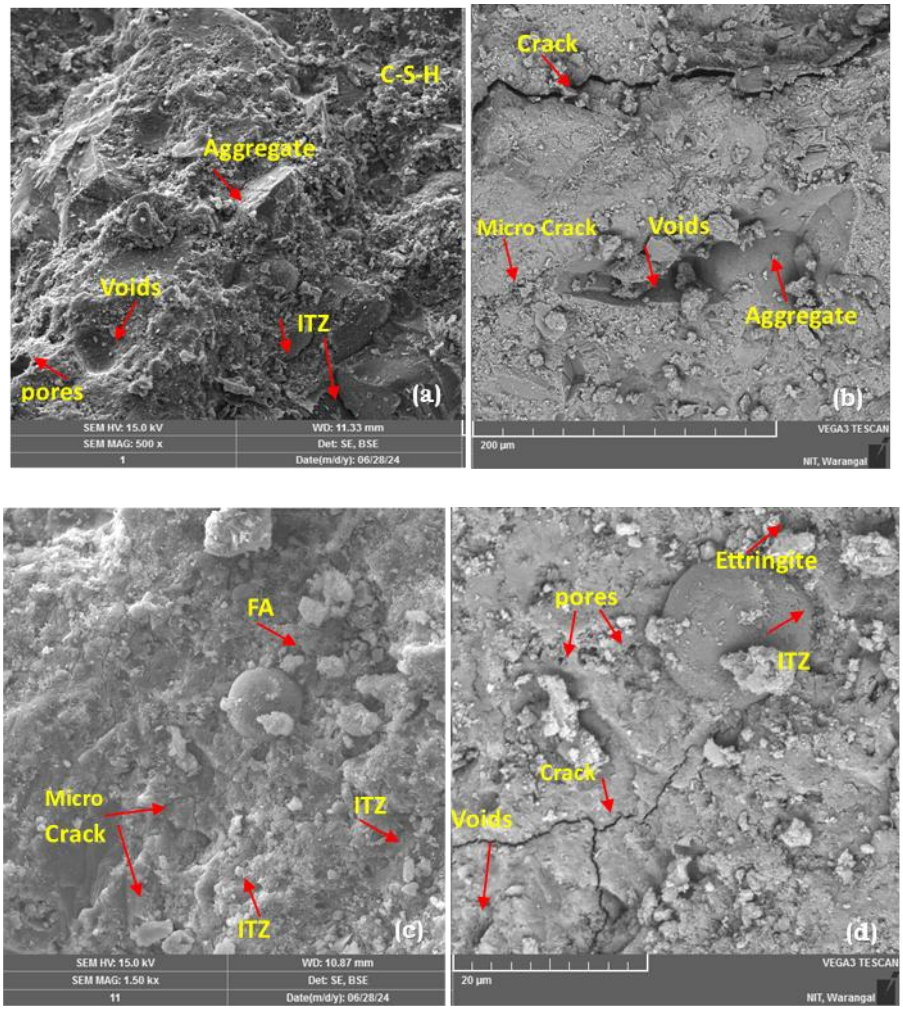

Fig. 36. SEM image of control concrete sample

4.7.2 Recycled Aggregate concrete

The concrete sample with recycled aggregate showed a irregular matrix surface with large number of voids, micro cracks and irregular glossy C-S-H gel and rod/needle shaped ettringites. The bonding between the aggregate and matrix sowed large number of cracks due to the replacement f recycled aggregate and poor bond between the old mortar and the new mortar layers. The ITZ zone showed lower strength due to wide cracks, making the zone weak and susceptible to cracking [76]. The numer of pores

and cracks are more prominent in recycled concrete samples with 50% recycled aggregate **(Fig. 37 a-b)**. The SEM image of the recycled aggregate concrete with 50% aggregate showed the presence of micro cracks and ettringites with voids and pores between the ITZ and aggregate. The diameter of void was large due to incomplete hydration products and excess shrinkage cracking . The SEM image of RAC50% sample with large dimeter voids and ettringites is shown in the **Fig. 37 (c&d)**. The ITZ zone exhibit lower strength and low modulus of elasticity which result in the reduction of the strength properties of concrete.

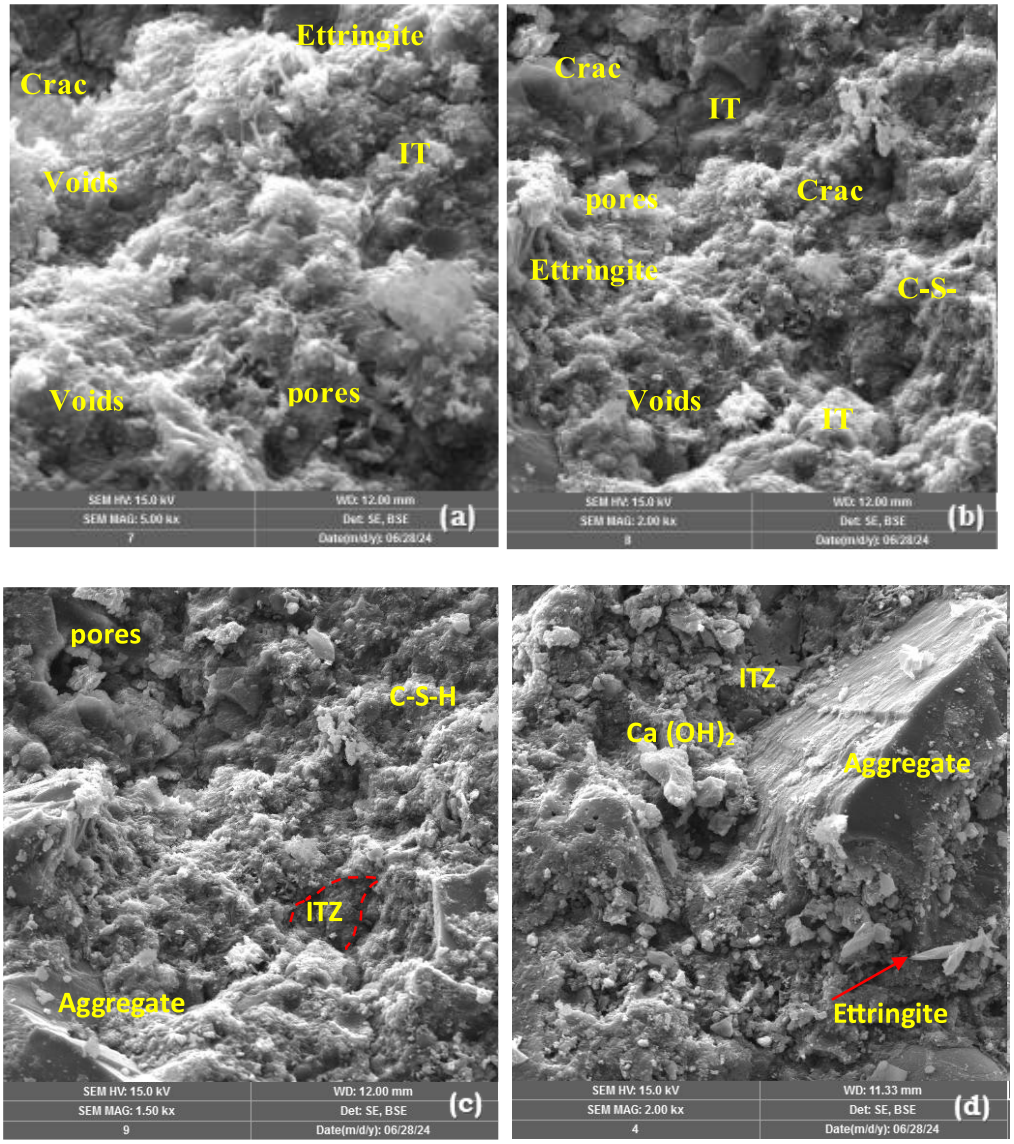

Fig. 37 SEM image of Recycled Aggregate Concrete (a-d) RAC 25%; (e-f) RAC 50%

4.7.3 Recycled aggregate concrete with plastic fibers (RAC 50%-PF 0.5%)

Addition of fibers to the concrete helps to change the pore structure of concrete and control the cracking behaviour. The quality and size and distribution of the hydration products depend upon the orientation and distribution of fibers in the concrete matrix. As the crack develops in the mortar, cracks tend to develop and propagate further with the increasing load [77]. As the crack reaches the fibers, the propagation of crack is restricted and the stress concentration is diminished by the presence of fibers. The fibers carry and transfer the load by the bonding with the cement concrete matrix. The fibers bridge the crack by anchorage with the mortar and prevent the crack propagation by bridging effect [28]. As the load further increase the fibers tends to pullout from the matrix and rupture at the ends, while the remining portion of the fibers is still fixed to the mortar. The size orientation, fold of the fibers plays

different role in arresting the cracks. The wider and long crack moves away from the fiber path. Scratches are formed when the fibers are subjected to excess stress and pulled out from the cement matrix [78]. The hydration products sticking on to the surface of fibers increases the bond between the fiber and mortar matrix [16]. Thus, the presence of fibers tends to improve the quality and orientation of the hydration product and reduces the cracks at the micro level. The SEM image of recycled aggregate concrete with plastic fiber is shown in **Fig. 38 (a-d)**. The incorporation of fibers in the concrete reduces the matrix's free shrinkage deformation, altering the orientation and quantity of hydration products. This, in turn, reduces the width of cracks at the coarse aggregate-matrix interface, enhancing the density of the concrete's aggregate interface transition zone.

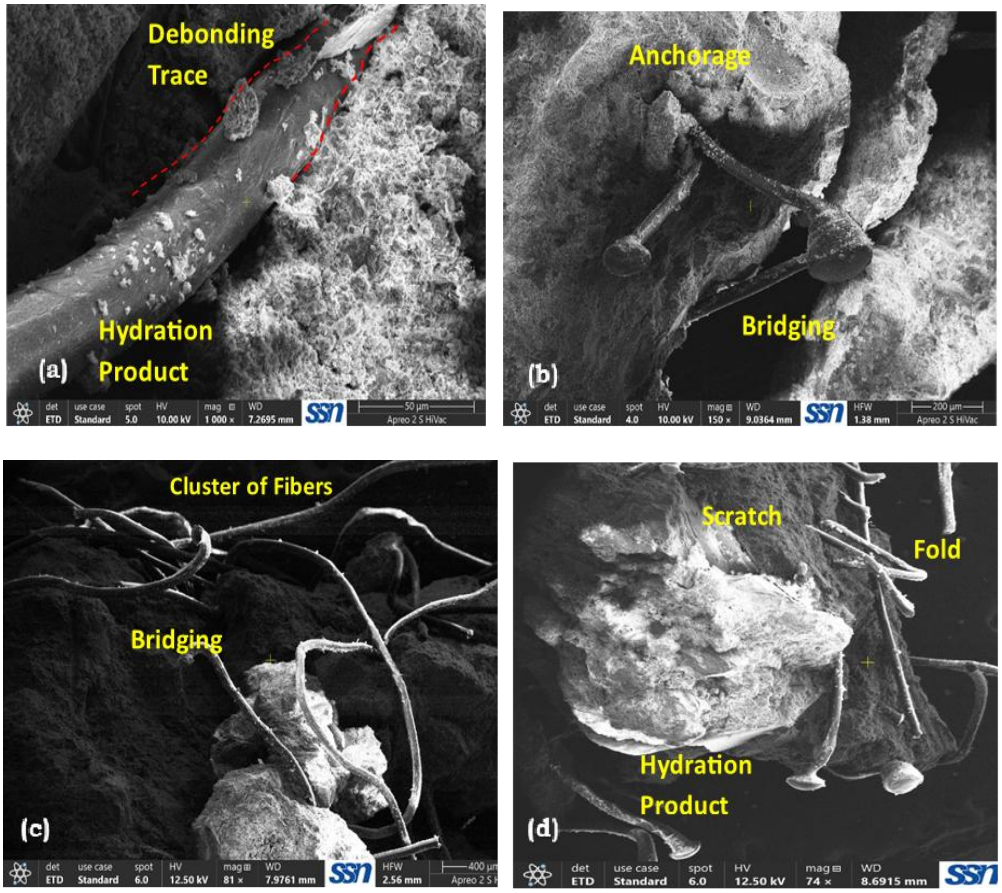

Fig. 38 SEM Image of RAC with plastic fiber

4.7.4 Recycled aggregate concrete with Hybrid fibers

The incorporation of plastic and polypropylene fibers tends to increase the number of micro cracks and reduces the size of macro cracks. Inclusion of micro and macro fibers densifies the concrete matrix and increases the compactness of the aggregate-cement matrix interface transition zone and reduces the formation of wide crack [78]. Beyond the indirect effect of fibers, it also reduces the crack formation by the bridging effect which improves the tensile property of concrete [77]. The surface of fibers is coated with the hydration products which helps to improve the bond between the fibers and cement matrix. The presence of fibers intercepts the distribution of solid particles and this leads to the accumulation low density hydration product near the fibers. The SEM image (**Fig. 39(a)**) shows the interlocking mechanism provided by the micro polypropylene fibers. The bridging effect provided by the micro fibers enhances the distribution of stress across the cement mortar matrix [79]. A dense C-H-S gel formation was observed in hybrid fiber reinforced mortar matrix **Fig. 39(b)**. As the stress in the micro fiber exceeds the fibers tends to rupture resulting in a frictional force between the fiber and matrix which results in the formation of scratches on the concrete surface. The incomplete hydration product formed on the surface of fibers creates a weak matrix interface zone [76]. As the stress exceeds the

strength of fibers the fibers tend to rupture and dissipate the stress in different direction. The SEM image of hybrid fiber reinforced recycled aggregate concrete is shown in **Fig. 39(a-d)**. The fibrillated nature of the polypropylene fibers takes he maximum stress while arresting the cracks and pulled out from the matrix shown a strong bond between fiber and mortar matrix. While rupture the fibers tends to fold/bend and contribute to the energy dissipation and prolong the wide crack formation by the matrix.

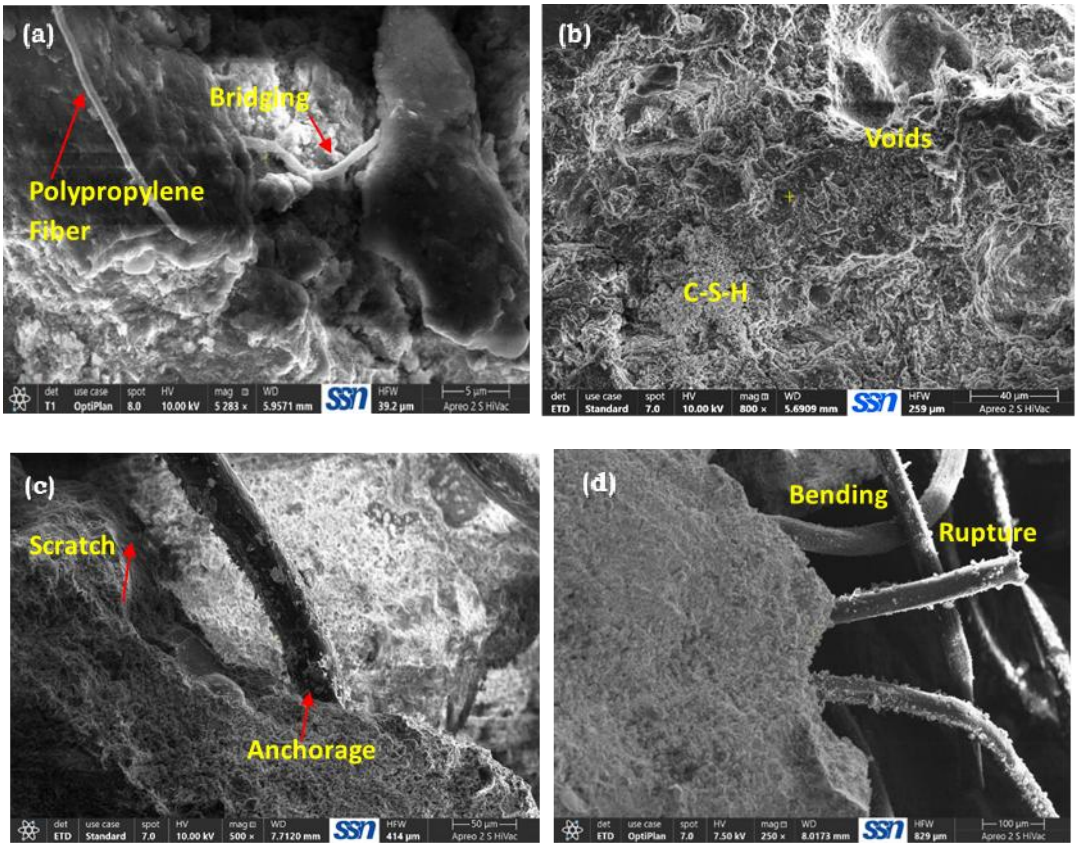

Fig. 39. SEM image of hybrid fiber reinforced recycled aggregate concrete

5 Conclusion

This research work reported on the experimental investigation, image processing and micro structural SEM image analysis of macro plastic , micro polypropylene and hybrid fiber reinforced recycled aggregate concrete. The stress strain plot and mechanical properties were thoroughly investigated for 50% for recycled aggregate concrete and the following conclusion were derived:

For the control and RAC specimen, brittle mode of failure of concrete was observed. With the addition of plastic fibers, the macro cracks were arrested and the shear failure behaviour was observed. In hybrid fiber RAC, the plastic fibers with high modulus of elasticity arrest the macro cracks and the polypropylene fibers arrest the micro cracks and help in bridging the major crack plane and the shear failure mode was observed.

For different proportions of Recycled Aggregate (RA) replacement rate it was observed that the mechanical strength decreases with the increase in dosage. The Recycled Aggregate (RA) reduces the modulus of elasticity of the concrete. For 25%, 50%, 75% and 100% RAC, the peak load carrying capacity reduces by 4%, 7% 11%, and 16% compared to normal concrete.

When compared to conventional concrete, RAC mixtures, especially those modified with PF and PP, demonstrate superior performance in sound absorption without compromising structural efficiency. Overall, modified RAC, particularly with fiber and polymer additives, proves to be a better alternative to conventional concrete for applications where sound absorption is a priority.

The Digital Image analysis carried out using the grey scale images, reveals the role of fibers in arresting micro and macro cracks using edge detection. The accumulation of polypropylene fibers

results in the formation of minute secondary cracks around the weak zone. The color pattern around the weak zone reveals the presence of fibers and its role in arresting micro cracks.

The concrete sample with recycled aggregate showed a irregular matrix surface with large number of voids, micro cracks and irregular glossy C-S-H gel and rod/needle shaped ettringites. SEM image analysis indicates that macro fibers arrest cracks at the initial stage, developing a dense cement mortar matrix during the hydration process, which aids in stress distribution. The combination of micro and macro fibers promotes the cement hydration process and forms a dense microstructure.

The results indicate that it is viable to develop environmentally sustainable fiber-reinforced recycled aggregate concrete (RAC) incorporating plastic and polypropylene fibers for structural use. Plastic fibers, functioning as macro-scale reinforcements with high stiffness, are particularly effective in bridging major cracks and enhancing overall strength. In contrast, polypropylene fibers, due to their micro-scale characteristics, play a key role in minimizing early-age plastic shrinkage and significantly improving post-cracking performance. However, this experimental investigation was limited to two levels of recycled aggregate replacement. Future studies could broaden the scope by exploring a full range of replacement ratios up to 100% and varying fiber dosages to optimize the design of a more robust and sustainable fiber-reinforced concrete system.

Acknowledgement

The author would like to acknowledge the support provided by the management of Sri Sivasubramaniya Nadar College of Engineering, Department of Civil Engineering, for facilitating this investigation at the Advanced Material Testing Laboratory. Additionally, the author extends gratitude to the Research Centre at Sri Sivasubramaniya Nadar College of Engineering, Department of EEE, for providing the microstructural FESEM image data.

Funding Statement

The author(s) received no specific funding for this study.

CRediT authorship contribution statement

Vijayalakshmi. Ramalingam: Investigation, Data Curation, Formal analysis, Writing -Original Draft. **Aswin Sriram :** Investigation, Data Curation, Formal analysis. **Geetha Ramalingam**: Investigation, Digital Image analysis, SEM image analysis. **Divyah Nagarajan**: Writing- Acoustic Emission Study, Review & Editing. **Prakash Ramaiah**: Review & Editing, Validation.

Conflicts of Interest

The authors declare that they have no conflicts of interest to report regarding the present study.

Data Availability Statement

Some or all data, models, or codes that support the findings of this study are available from the corresponding author upon reasonable request.

References

[1] Bayrak B, Benli A, Alcan HG, Çelebi O, Kaplan G, Aydın AC. Recycling of waste marble powder and waste colemanite in ternary-blended green geopolymer composites: Mechanical, durability and microstructural properties. Journal of Building Engineering 2023; 73: 106661. https://doi.org/10.1016/j.jobe.2023.106661.

[2] Vahidi A, Mostaani A, Gebremariam AT, Di Maio F, Rem P. Feasibility of utilizing recycled coarse aggregates in commercial concrete production. Journal of Cleaner Production 2024; 474: 143578. https://doi.org/10.1016/j.jclepro.2024.143578.

[3] Tejas S, Pasla D. Approach to design sustainable alkali-activated slag recycled aggregate concrete: Mechanical and microstructural characterization. Case Studies in Construction Materials 2024; 21: e03886. https://doi.org/10.1016/j.cscm.2024.e03886.

[4] Sae-Long W, et al. Experimental and simulation analysis of RCA and para-wood ash as partial substitutes for NCA and cement in recycled aggregate concrete. Case Studies in Construction Materials 2024; 21:

e03716. https://doi.org/10.1016/j.cscm.2024.e03716.
[5] Forero JA, de Brito J, Evangelista L, Pereira CHF. Mechanical and fracture properties of concrete with recycled concrete aggregates treated with acids and addition of aluminium sulphate. Construction and Building Materials 2024; 447: 137947. https://doi.org/10.1016/j.conbuildmat.2024.137947.
[6] Raza A, et al. Mechanical, durability, and microstructural evaluation of coal ash incorporated recycled aggregate concrete: An application of waste effluents for sustainable construction. Buildings 2022; 12(10): 1715. https://doi.org/10.3390/buildings12101715.
[7] Jin L, Wu T, Liu P, Wang Z, Zhou P. Macro–meso degradation evolution of fully recycled coarse aggregate concrete under sulfate attack in marine environment. Structures 2024; 69: 107536. https://doi.org/10.1016/j.istruc.2024.107536.
[8] Zhu P, Chen X, Liu H, Wang Z, Chen C, Li H. Recycling of waste recycled aggregate concrete in freeze-thaw environment and emergy analysis of concrete recycling system. Journal of Building Engineering 2024; 96: 110377. https://doi.org/10.1016/j.jobe.2024.110377.
[9] Caracol C, Kravchanka L, Bravo M, de Brito J, Agrela F, Rosales J. Recycled aggregate concrete using seawater: Optimizing concrete's sustainability. Journal of Building Engineering 2024; 97: 110841. https://doi.org/10.1016/j.jobe.2024.110841.
[10] Htet P, Chen W, Huang Z, Hao H. Physical and mechanical properties of deflection-hardening hybrid fibre-reinforced recycled aggregate concrete. Journal of Building Engineering 2024; 90: 109510. https://doi.org/10.1016/j.jobe.2024.109510.
[11] Kaplan G, Coskan U, Benli A, Bayraktar OY, Kucukbaltacı AB. The impact of natural and calcined zeolites on the mechanical and durability characteristics of glass fiber reinforced cement composites. Construction and Building Materials 2021; 311: 125336. https://doi.org/10.1016/j.conbuildmat.2021.125336.
[12] Sathia R, Vijayalakshmi R. Fresh and mechanical property of Caryota urens fiber reinforced flowable concrete. Journal of Materials Research and Technology 2021; 15: 3647–3662. https://doi.org/10.1016/j. jmrt.2021.09.126.
[13] Vijayalakshmi R, Sriram AG, Prakash R, Divyah N, Geetha R. Micro structure analysis and digital image processing of monofilament and fibrillated fiber reinforced recycled aggregate concrete. Structural Engineering and Mechanics 2025; 1: 65–89.
[14] Yu Y, Zhou L, Liao Z, Zheng Y. Tension stiffening and cracking behaviors in glass fiber reinforced polymer bar enhanced precast recycled aggregate concrete specimen. Structures 2024; 69: 107395. https://doi.org/10.1016/j.istruc.2024.107395.
[15] Jamil K, Shabbir F, Raza A. Performance evaluation of jute fiber-reinforced recycled aggregate concrete: Strength and durability aspects. Structural Concrete 2023; 24(5): 6520–6538. https://doi.org/10.1002/suco.202200948.
[16] Raza A, Ahmed B, El Ouni MH, Chen W. Mechanical, durability and microstructural characterization of cost-effective polyethylene fiber-reinforced geopolymer concrete. Construction and Building Materials 2024; 432: 136661. https://doi.org/10.1016/j.conbuildmat.2024.136661.
[17] Carneiro JA, Lima PRL, Leite MB, Toledo Filho RD. Compressive stress–strain behavior of steel fiber reinforced recycled aggregate concrete. Cement and Concrete Composites 2014; 46: 65–72. https://doi.org/10.1016/j.cemconcomp.2013.11.006.
[18] W, et al. Mechanical properties and constitutive relation of recycled aggregate concrete reinforced with face mask fibre and basalt fibre under uniaxial cyclic compression. Structures 2024; 69: 107364. https://doi.org/10.1016/j.istruc.2024.107364.
[19] Guler S, Öker B, Akbulut ZF. Workability, strength and toughness properties of different types of fiber-reinforced wet-mix shotcrete. Structures 2021; 31: 781–791. https://doi.org/10.1016/j.istruc.2021.02.031.
[20] Vijayalakshmi R, et al. Fresh and hardened property of fish tail palm fiber reinforced concrete: Effect of fiber content and fiber length. European Journal of Environmental and Civil Engineering 2022; 1–19. https://doi.org/10.1080/19648189.2022.2086178.
[21] Ramalingam S, Ramalingam V, Srinivasan R, Gopinath V, Ramanareddy Y, Ramanareddy Y. Uni axial compression behaviour of lightweight expanded clay aggregate concrete cylinders confined by perforated steel tube and GFRP wrapping. Revista de la Construcción. Journal of Construction 2020; 19(3): 200–212. https://doi.org/10.7764/rdlc.19.3.200-212. revistadelaconstruccion.uc.cl
[22] Sriram M, Sidhaarth KRA. Influence of silica fume and metakaolin on durability properties of hybrid fibers reinforced high strength concrete. Journal of Building Pathology and Rehabilitation 2023; 8(1): 1–13. https://doi.org/10.1007/s41024-023-00266-6.
[23] Xiong Z, et al. Fracture properties and mechanisms of steel fiber and glass fiber reinforced rubberized concrete. Journal of Building Engineering 2024; 86: 108866. https://doi.org/10.1016/j.jobe.2024.108866.
[24] Pereiro-Barceló J, Lenz E, Torres B, Estevan L. Mechanical properties of recycled aggregate concrete reinforced with conventional and recycled steel fibers and exposed to high temperatures. Construction and Building Materials 2024; 452: 138976. https://doi.org/10.1016/j.conbuildmat.2024.138976.

[25] Htet P, Chen W, Hao H, Li Z, Shaikh F. Hybrid fibre reinforced recycled aggregate concrete: Dynamic mechanical properties and durability. Construction and Building Materials 2024; 415: 135044. https://doi.org/10.1016/j.conbuildmat.2024.135044.
[26] Bao S, Wang S, Xia H, Liu K, Tang X, Jin P. Enhancing the mechanical properties of recycled aggregate concrete: A comparative study of basalt- and glass-fiber reinforcements. Buildings 2025; 15(10): 1718. https://doi.org/10.3390/buildings15101718.
[27] Zhang X, Wang J, Lou C. Experimental study on axial tensile properties of basalt fibre reinforced recycled aggregate concrete. Heliyon 2024; 10(13): e34208. https://doi.org/10.1016/j.heliyon.2024.e34208.
[28] Zhong C, et al. Experimental investigation on flexural fatigue performance of recycled aggregate concrete hybrid with basalt-polyacrylonitrile fiber. Scientific Reports 2025; 15(1): 5855. https://doi.org/10.1038/ s41598-025-89682-x.
[29] Mishra S, Goel R. A comparison of treated recycled aggregate concrete, natural aggregate, and recycled aggregate concrete using improved RCA surface treatment. Journal of Information Systems Engineering and Management 2025; 10(48s): 1381–1392. Available: https://jisem-journal.com/
[30] Islam SR, Mutsuddy R, Shahid NB. Gray correlation coefficient analysis on the mechanical properties of nylon fiber reinforced recycled aggregate concrete with GGBS. Civil Engineering Journal 2025; 11(3): 932–949. https://doi.org/10.28991/CEJ-2025-011-03-07.
[31] Zhou B, Zhang M, Ma G. An experimental study on 3D printed concrete reinforced with fibers recycled from wind turbine blades. Journal of Building Engineering 2024; 91: 109578. https://doi.org/10.1016/j.jobe.2024.109578.
[32] Zhang L, He M, Li X, Li C, Zhao J, Wang HC. Experimental and model calculation research on shrinkage of hybrid fiber-reinforced recycled aggregate concrete. Materials (Basel) 2025; 18(5): 1183. https://doi.org/10.3390/ma18051183.
[33] Li H, Wei Y, Meng K, Zhao L, Zhu B, Wei B. Mechanical properties and stress-strain relationship of surface-treated bamboo fiber reinforced lightweight aggregate concrete. Construction and Building Materials 2024; 424: 135914. https://doi.org/10.1016/j.conbuildmat.2024.135914.
[34] Feng J, Jia X, Dong X, Wang P, Xu B, Wang Z. Cyclic compressive behavior of hook-end steel and macro-polypropylene hybrid fiber reinforced recycled aggregate concrete. Case Studies in Construction Materials 2023; 19: e02310. https://doi.org/10.1016/j.cscm.2023.e02310.
[35] Cui K, et al. Mechanical behavior of multiscale hybrid fiber reinforced recycled aggregate concrete subject to uniaxial compression. Journal of Building Engineering 2023; 71: 106504. https://doi.org/10.1016/j.jobe.2023.106504.
[36] Tahir M, Hameed R, Riaz MR, Waqas M. Bond stress-slip behavior of hybrid fiber-reinforced recycled aggregate concrete using beam test. Iranian Journal of Science and Technology, Transactions of Civil Engineering 2023; 47(2): 753–760. https://doi.org/10.1007/s40996-023-01042-9.
[37] Zia A, Ali M. Behavior of fiber reinforced concrete for controlling the rate of cracking in canal-lining. Construction and Building Materials 2017; 155: 726–739. https://doi.org/10.1016/j.conbuildmat.2017.08.078.
[38] Fu B, Xu GT, Peng WS, Huang JZ, Zou QQ, Kuang YD. Performance enhancement of recycled coarse aggregate concrete by incorporating with macro fibers processed from waste GFRP. Construction and Building Materials 2024; 411: 134166. https://doi.org/10.1016/j.conbuildmat.2023.134166.
[39] Bureau of Indian Standards. Method of test for strength of concrete (IS 516:2014). BIS, New Delhi, 2014.
[40] Bureau of Indian Standards. Splitting tensile strength of concrete—Method of test (IS 5816:1999, First revision). BIS, New Delhi, 1999.
[41] Garai M, Pompoli F. A simple empirical model of polyester fibre materials for acoustical applications. Applied Acoustics 2005; 66(12): 1383–1398. https://doi.org/10.1016/j.apacoust.2005.04.008.
[42] Ley MT, Welchel D, Peery J, LeFlore J. Determining the air-void distribution in fresh concrete with the sequential air method. Construction and Building Materials 2017; 150: 723–737. https://doi.org/10.1016/j.conbuildmat.2017.06.037.
[43] Wu H, Zhang J, Chen Y, Jiang R, Zhu Z, Li P. Stress-strain behavior and failure criterion study of polypropylene fiber reinforced recycled aggregate concrete under triaxial stress state. Construction and Building Materials 2024; 448: 138185. https://doi.org/10.1016/j.conbuildmat.2024.138185.
[44] Gao H, et al. Cyclic compressive behavior of high-performance hybrid fiber reinforced recycled aggregate concrete: Degradation law and acoustic emission features. Construction and Building Materials 2024; 431: 136412. https://doi.org/10.1016/j.conbuildmat.2024.136412.
[45] El Ouni MH, et al. Mechanical performance, water and chloride permeability of hybrid steel-polypropylene fiber-reinforced recycled aggregate concrete. Case Studies in Construction Materials 2022; 16: e00831. https://doi.org/10.1016/j.cscm.2021.e00831.
[46] Yang J, Du Q, Bao Y. Concrete with recycled concrete aggregate and crushed clay bricks. Construction and Building Materials 2011; 25(4): 1935–1945. https://doi.org/10.1016/j.conbuildmat.2010.11.063.

[47] Akça KIR, Çakir Ö, Ipek M. Properties of polypropylene fiber reinforced concrete using recycled aggregates. Construction and Building Materials 2015; 98: 620–630. https://doi.org/10.1016/j.conbuildmat.2015.08.133.
[48] Chen S, Liu Y, Bie Y, Duan P, Wang L. Multi-scale performance study of concrete with recycled aggregate from tannery sludge. Case Studies in Construction Materials 2022; 17: e01698. https://doi.org/10.1016/j.cscm.2022.e01698.
[49] Alqahtani FK, Abotaleb IS, ElMenshawy M. Life cycle cost analysis of lightweight green concrete utilizing recycled plastic aggregates. Journal of Building Engineering 2021; 40: 102670. https://doi.org/10.1016/j.jobe.2021.102670.
[50] Zhang X, et al. Compressive mechanical performance and microscopic mechanism of basalt fiber-reinforced recycled aggregate concrete after elevated temperature exposure. Journal of Building Engineering 2024; 96: 110647. https://doi.org/10.1016/j.jobe.2024.110647.
[51] Bayraktar OY, Eshtewı SE, Benli A, Kaplan G, Toklu K, Gunek F. The impact of RCA and fly ash on the mechanical and durability properties of polypropylene fibre-reinforced concrete exposed to freeze-thaw cycles and MgSO4 with ANN modeling. Construction and Building Materials 2021; 313: 125508. https://doi.org/10.1016/j.conbuildmat.2021.125508.
[52] Manoharan M, Sivakumar VL, Priya MG, Arthi AJJ, Hasan NMU. Augmented properties of high strength self-compaction concrete partially replaced with nano mineral admixtures. SSRG International Journal of Civil Engineering 2023; 10(9): 11–21. https://doi.org/10.14445/23488352/IJCE-V10I9P102.
[53] Bayraktar OY, Bozkurt TH, Benli A, Koksal F, Türkoğlu M, Kaplan G. Sustainable one-part alkali activated slag/fly ash Geo-SIFCOM containing recycled sands: Mechanical, flexural, durability and microstructural properties. Sustainable Chemistry and Pharmacy 2023; 36: 101319. https://doi.org/10.1016/j.scp.2023.101319.
[54] Abdallah S, Rees DWA, Ghaffar SH, Fan M. Understanding the effects of hooked-end steel fibre geometry on the uniaxial tensile behaviour of self-compacting concrete. Construction and Building Materials 2018; 178: 484–494. https://doi.org/10.1016/j.conbuildmat.2018.05.191.
[55] Patil GM, Prakash SS. Effect of macro-synthetic and hybrid fibres on the behaviour of square concrete columns reinforced with GFRP rebars under eccentric compression. Structures 2024; 59: 105707. https://doi.org/10.1016/j.istruc.2023.105707.
[56] Zhang K, Lin W, Lan Q, Zhang Q. Compressive properties of polypropylene fiber reinforced seawater sea-sand recycled aggregate concrete under different strain rate loading. Construction and Building Materials 2024; 452: 138968. https://doi.org/10.1016/j.conbuildmat.2024.138968.
[57] Zhang X, et al. Experimental study on impact resistance and dynamic constitutive relation of steel fiber reinforced recycled aggregate concrete. Construction and Building Materials 2024; 449: 138396. https://doi.org/10.1016/j.conbuildmat.2024.138396.
[58] Koksal F, Bacanli C, Benli A, Gencel O. Fresh, flexural and mechanical performance of polyamide and polypropylene based macro-synthetic fiber-reinforced concretes. Structural Engineering and Mechanics 2022; 82(1): 93–105. https://doi.org/10.12989/sem.2022.82.1.093.
[59] Krishnan R, Sivakumar VL, Manigandan R. Investigation on the effect of axial compression on rectangular multi-partition steel-concrete composite walls with stiffeners. Structures 2025; 71: 108055. https://doi.org/10.1016/j.istruc.2024.108055.
[60] Krishnan R, Sivakumar VL. The effect of soil-structure interaction (SSI) on structural stability and sustainability of RC structures. Civil and Environmental Engineering Reports 2024; 34(1): 47–67. https://doi.org/10.59440/ceer/184254.
[61] American Concrete Institute. Building code requirements for structural concrete and commentary (ACI 318-11). ACI, USA, 2011.
[62] British Standards Institution. Eurocode 2: Design of concrete structures—Part 1-1: General rules and rules for buildings (EN 1992-1-1). BSI, 2004.
[63] Japan Concrete Institute. Guideline for control of cracking of mass concrete. JCI, Japan, 2008.
[64] Standards New Zealand. Concrete structures standard—NZS 3101: The design of concrete structures. New Zealand, 2006.
[65] Kumari J, Rao MVS, Sina S, Reddy VS. Hybrid steel/glass fiber-reinforced self-consolidating concrete considering packing factor: Mechanical and durability characteristics. Structures 2020; 28: 956–972. https://doi.org/10.1016/j.istruc.2020.09.042.
[66] Azandariani MG, Vajdian M, Javadi M, Parvari A. Durability and compressive strength of composite polyolefin fiber-reinforced recycled aggregate concrete: An experimental study. Composites Part C: Open Access 2024; 15: 100533. https://doi.org/10.1016/j.jcomc.2024.100533
[67] Zhang H, Cao L, Duan Y, Tang Z, Hu F, Chen Z. High-flowable and high-performance steel fiber reinforced concrete adapted by fly ash and silica fume. Case Studies in Construction Materials 2024; 20: e02796. https://doi.org/10.1016/j.cscm.2023.e02796.
[68] Wang C, Yuan J, Zhang Y, Ma Z. Study on the mesoscopic mechanical behavior and damage constitutive

model of micro-steel fiber reinforced recycled aggregate concrete. Construction and Building Materials 2024; 443: 137767. https://doi.org/10.1016/j.conbuildmat.2024.137767.

[69] Jiao Y, Du W, Yang H, Shi H. Low temperature failure behavior analysis of fiber reinforced asphalt concrete under indirect tension test using acoustic emission and digital image correlation. Case Studies in Construction Materials 2024; 20: e02720. https://doi.org/10.1016/j.cscm.2023.e02720.

[70] Rimkus A, Podviezko A, Gribniak V. Processing digital images for crack localization in reinforced concrete members. Procedia Engineering 2015; 122: 239–243. https://doi.org/10.1016/j.proeng.2015.10.031.

[71] Ikumi T, Pujadas P, de la Cruz J, Segura I, de la Fuente A. Modified digital image correlation aided measurement of the transverse to longitudinal deformation ratio for polymeric macro-fibres. Materials & Design 2022; 223: 111164. https://doi.org/10.1016/j.matdes.2022.111164.

[72] Lu Y, Duanmu L, Zhai ZJ, Wang Z. Application and improvement of Canny edge-detection algorithm for exterior wall hollowing detection using infrared thermal images. Energy and Buildings 2022; 274: 112421. https://doi.org/10.1016/j.enbuild.2022.112421.

[73] Mahakavi P, Chithra R. Impact resistance, microstructures and digital image processing on self-compacting concrete with hooked end and crimped steel fiber. Construction and Building Materials 2019; 220: 651–666. https://doi.org/10.1016/j.conbuildmat.2019.06.001.

[74] Li X, Lin H, Chen W, Liang S, Huang L. A numerical study on the tensile splitting of concrete with digital image processing. Journal of Materials Research and Technology 2023; 25: 1626–1641. https://doi.org/10.1016/j.jmrt.2023.06.026.

[75] Abouelnour MA, EL-Aziz MAA, Osman KM, Fathy IN, Tayeh BA, Elfakharany ME. Recycling of marble and granite waste in concrete by incorporating nano alumina. Construction and Building Materials 2024; 411: 134456. https://doi.org/10.1016/j.conbuildmat.2023.134456.

[76] Quan P, et al. Study on the mechanical properties and strength formation mechanism of high-volume graphite tailings concrete. Journal of Building Engineering 2024; 84: 108500. https://doi.org/10.1016/j.jobe.2024.108500.

[77] Zhou M, He X, Wang H, Wu C, He J, Wei B. Mechanical properties and microstructure of ITZs in steel and polypropylene hybrid fiber-reinforced concrete. Construction and Building Materials 2024; 415: 135119. https://doi.org/10.1016/j.conbuildmat.2024.135119.

[78] Masoud L, Hammoud A, Mortada Y, Masad E. Rheological, mechanical, and microscopic properties of polypropylene fiber reinforced-geopolymer concrete for additive manufacturing. Construction and Building Materials 2024; 438: 137069. https://doi.org/10.1016/j.conbuildmat.2024.137069.

[79] Zhao T, Song P, Dong G, Lv Y, Sun M, Chen J. Experimental research and theoretical prediction on mechanical properties for recycled GFRP fiber reinforced concrete. Journal of Building Engineering 2024; 91: 109643. https://doi.org/10.1016/j.jobe.2024.109643.

[80] Liang N, Geng S, Mao J, Liu X, Zhou X. Investigation on cracking resistance mechanism of basalt-polypropylene fiber reinforced concrete based on SEM test. Construction and Building Materials 2024; 411: 134102. https://doi.org/10.1016/j.conbuildmat.2023.134102